2 | The Two-Nucleon System

2.1 Introduction

The study of the hydrogen atom is relatively simple due the fact that the Coulomb force between the proton and the electron is very well known. The solution of this quantum problem resulted in the determination of a group of states of energy allowed for the system, permitting direct comparison with the measured values of the electromagnetic transitions between those states. Ever since, there has been great progress in understanding the hydrogen atom and atoms with many electrons. Nowadays, there are only small discrepancies between quantum theory and experimental data.

Nuclear systems are much more complex than atomic ones. Already the simplest case, the system of two nucleons, has its theoretical treatment hindered by the fact that the form of the force acting between them is not well known. In spite of that, quantum theory has been used with success in several areas of nuclear physics. In this chapter we will make a simple application of it to the system of two nucleons and an expression will be presented for their interaction potential.

Two groups of experimental data exist for the system of two nucleons. A first group arises from the study of the only bound system of that kind, the deuteron, composed of a proton and a neutron. Unlike the hydrogen atom, the deuteron has only one bound state, the ground state. Therefore, the theories for the neutron-proton interaction in the deuteron can only be tested by comparing their predictions with the experimental values of the energy, angular momentum, parity, magnetic dipole moment, and electric quadrupole moment of the ground state of the deuteron.

The second group of experimental data come from the study of nucleon-nucleon scattering. As it is difficult to produce a neutron beam for that goal (the neutrons have zero charge and cannot be accelerated by means of an electric field), the experiments are limited to collisions between protons and to proton-deuteron scattering, this last supplying indirect information on proton-neutron interaction. Comparison of the experimental data for those collisions and the properties of the ground state of the deuteron has been useful

for the semi-phenomenological description of the interaction between two nucleons, as we shall see below.

2.2 Electrostatic Multipoles

Electromagnetic multipoles give one of the most important examples of tensor operators. They appear in classical field theory as a result of the *multipole expansion* of the fields created by a finite system of charges and currents. We start with the system of point-like classical particles with electric charges e_a located at the points $\mathbf{r}_a$. If you are not used to angular momentum algebra, read Appendices A and B first.

The electrostatic potential of this system measured at the point $\mathbf{r}$ is given by the Coulomb law,

$$\phi(\mathbf{r}) = \sum_a \frac{e_a}{|\mathbf{r} - \mathbf{r}_a|}. \tag{2.1}$$

The function

$$\frac{1}{|\mathbf{r} - \mathbf{r}'|} = \frac{1}{\sqrt{r^2 + r'^2 - 2rr' \cos\gamma}} \tag{2.2}$$

depends on the lengths r, r' of two vectors and the angle γ between them rather than on the angles of the vectors $\mathbf{r}$ and $\mathbf{r}'$ separately. If $\mathbf{r} \neq \mathbf{r}'$, this function has no singularities and can be expressed with the aid of the expansion over the infinite set of Legendre polynomials with coefficients depending on r and r',

$$\frac{1}{|\mathbf{r} - \mathbf{r}'|} = \sum_{l=0}^{\infty} P_l(\cos\gamma) f_l(r, r'). \tag{2.3}$$

Using the notation $r_<$ and $r_>$ for the smaller and greater r and r', one can show that the expansion (2.3) takes the form

$$\frac{1}{|\mathbf{r} - \mathbf{r}'|} = \sum_l \frac{r_<^l}{r_>^{l+1}} P_l(\cos\gamma). \tag{2.4}$$

The applications of the multipole expansion usually consider the potential (2.1) *outside the system*, that is, at the point r with $r > r_a$. Then we can use the expansion (2.4) and the *addition theorem* (A.112) to get

$$\phi(\mathbf{r}) = \sum_{lm} \frac{4\pi}{2l + 1} \frac{1}{r^{l+1}} Y_{lm}^*(\mathbf{n}) \mathcal{M}(El, m). \tag{2.5}$$

Here the *electric multipole moment* of rank l, $l = 0, 1, \ldots$, is defined for a system of point-like charges $a = 1, 2, \ldots, A$ as a set of $2l + 1$ quantities,

$$\mathcal{M}(El, m) = \sum_a e_a r_a^l Y_{lm}(\mathbf{n}_a), \quad m = -l, -l+1, \ldots, +l, \tag{2.6}$$

where the sum runs over all charges e_a located at $\mathbf{r}_a = (r_a, \theta_a, \phi_a) \equiv (r_a, \mathbf{n}_a)$. Exactly in the same way one can define, instead of the charge distribution, multipole moments for any other property of the particles, for example, for the mass distribution, $e_a \to m_a$.

In quantum theory, multipole moments are to be considered as operators acting on the variables of the particles. Containing explicitly the spherical functions, the operator $\mathcal{M}(El, m)$ has the necessary features of the tensor operator of rank l. Introducing the *charge density* operator

$$\rho(\mathbf{r}) = \sum_a e_a \delta(\mathbf{r} - \mathbf{r}_a), \tag{2.7}$$

we come to a more general form of the multipole moment,

$$\mathcal{M}(El, m) = \int d^3r \, \rho(\mathbf{r}) r^l Y_{lm}(\mathbf{n}), \quad \mathbf{n} = \frac{\mathbf{r}}{r}. \tag{2.8}$$

In this form we do not even need to make an assumption of existence of point-like constituents in the system; for example, in the nucleus charged pions and other mediators of nuclear forces are included along with the nucleons if $\rho(\mathbf{r})$ is the total operator of electric charge density. As expected, we can separate the geometry of multipole operators from their dynamical origin. From any underlying structure $\rho(\mathbf{r})$, the operator (2.8) extracts the irreducible tensor of rank l, that is, the part with specific rotational properties.

The lowest multipole moment $l = 0$ is the *monopole* one. It determines the scalar part, the total electric charge Ze,

$$\mathcal{M}(E0, 0) = \frac{1}{\sqrt{4\pi}} \sum_a e_a = \frac{1}{\sqrt{4\pi}} \int d^3r \, \rho(\mathbf{r}) = \frac{1}{\sqrt{4\pi}} Ze. \tag{2.9}$$

The next term, $l = 1$, defines the vector of the *dipole* moment,

$$\mathbf{d} = \sum_a e_a \mathbf{r}_a = \int d^3r \, \rho(\mathbf{r}) \mathbf{r}. \tag{2.10}$$

Taking into account the relation (B.8) between the vectors and the spherical functions of rank $l = 1$, we obtain

$$\mathcal{M}(E1, m) = \sqrt{\frac{3}{4\pi}} \sum_a e_a r_a (n_a)_m = \sqrt{\frac{3}{4\pi}} d_m. \tag{2.11}$$

Subsequent terms of the multipole expansion determine the quadrupole ($l = 2$), *octupole* ($l = 3$), *hexadecapole* ($l = 4$), and higher moments. Physical properties of the quadrupole tensor, recall (B.12), play an important role in molecular and nuclear structure.

In a similar way one can define *magnetic multipoles* $\mathcal{M}(Ml, m)$ related to the distribution of currents. The convection current due to orbital motion and the magnetization current generated by the spin magnetic moments determine corresponding contributions to the magnetic multipole moment of rank l,

$$\mathcal{M}(Ml, m) = \sum_a \left(g_a^s \mathbf{s}_a + \frac{2}{l+1} g_a^l \mathbf{l}_a \right) \cdot \nabla(r_a^l Y_{lm}(\mathbf{n}_a)). \tag{2.12}$$

Here $\mathbf{s}_a$:
tively; g_a^s

momenta in units of $\hbar$ and the gyromagnetic ratios in the magnetons $e\hbar/(2m_a c)$.) The expression (2.12) vanishes for $l = 0$ demonstrating the absence of magnetic monopoles. At $l = 1$, we come to the spherical components μ_m, (B.8), of the *magnetic moment* μ,

$$\mathcal{M}(M1, m) = \sqrt{\frac{3}{4\pi}} \mu_m, \tag{2.13}$$

$$\mu = \sum_a (g_a^s \mathbf{s}_a + g_a^l \mathbf{l}_a). \tag{2.14}$$

Higher terms determine magnetic quadrupole, $l = 2$, magnetic octupole, $l = 3$, and so on.

2.3 Magnetic Moment with Spin-orbit Coupling

The vector model described in Appendix B will be used to study the magnetic moment with *spin-orbit coupling*. Let a particle with spin s move in a central field where its orbit is characterized by an orbital momentum l. The energy of the orbit depends in general on the mutual orientation of the quantum vectors $\mathbf{l}$ and $\mathbf{s}$. This spin-orbit interaction is rather weak $(\sim v^2/c^2)$ for electrons in atoms, although it becomes increasingly important in heavy atoms with a large nuclear charge Z, when the electrons reach relativistic velocities, $v/c \sim \alpha Z$, where $\alpha = e^2/\hbar c \approx 1/137$ is the *fine structure constant*. In light atoms one can use the *ls* coupling scheme when, analogously to the states $|j_1 m_1; j_2 m_2\rangle$ in (B.41), the electron state $|l l_z; s s_z\rangle$ is described separately by the constituent angular momenta $\mathbf{l}$ and $\mathbf{s}$. For nucleons in nuclei, the spin-orbit coupling is strong, and one has to introduce the total angular momentum of the nucleon

$$\mathbf{j} = \mathbf{l} + \mathbf{s} \tag{2.15}$$

and use the corresponding basis of states $|(ls)jj_z = m\rangle$.

Since the lengths of all vectors in (2.15) are fixed,

$$\mathbf{j}^2 = j(j+1), \quad \mathbf{l}^2 = l(l+1), \quad \mathbf{s}^2 = s(s+1), \tag{2.16}$$

(Equation 2.15) enables us to find the average mutual orientations

$$(\mathbf{j} \cdot \mathbf{l}) = \frac{j(j+1) + l(l+1) - s(s+1)}{2}, \quad (\mathbf{j} \cdot \mathbf{s}) = \frac{j(j+1) + s(s+1) - l(l+1)}{2}. \tag{2.17}$$

Of course, the scalar quantities (2.17) are the same for all the states $|(ls)jm\rangle$ with different m.

The operator of magnetic moment (2.14) of a particle in a central field is given (in units of the corresponding magneton)

$$\mu = g^s \mathbf{s} + g^l \mathbf{l}. \tag{2.18}$$

Using the vector model (B.51), (B.52) together with the scalar quantities (2.17), we obtain the *effective operator* of the magnetic moment within the multiplet of states $|jm\rangle$,

$$\mu = g(j, l, s)\mathbf{j}, \tag{2.19}$$

where the gyromagnetic ratio (*Landé factor*) is

$$g(j,l,s) = g^l \frac{\langle\langle j \cdot l \rangle\rangle}{j(j+1)} + g^s \frac{\langle\langle j \cdot s \rangle\rangle}{j(j+1)}$$

$$= \frac{1}{2j(j+1)} \{(g^l + g^s)j(j+1) + (g^l - g^s)[l(l+1) - s(s+1)]\}. \tag{2.20}$$

As we mentioned, the tabular value corresponds to the state with $j_z = j$, that is, the magnetic moment is equal to $\mu = gj$.

For a free nucleon at rest $l = 0$ and $j = s = \frac{1}{2}$. Therefore spin gyromagnetic ratios are determined by the empirical magnetic moments μ_p and μ_n,

$$g_p^s = 2\mu_p = 5.58, \quad g_n^s = 2\mu_n = -3.82. \tag{2.21}$$

(in nuclear magnetons). The spin gyromagnetic ratio is predicted by the relativistic Dirac equation (see Appendix D) to be equal to $g^s = 2$ for a structureless particle of spin $\frac{1}{2}$ and charge e (in units of the corresponding magneton). This would lead to the spin magnetic moment of a free particle being exactly one magneton. This is the case for the electron (or positron) with small QED corrections of order 10^{-3} due to vacuum polarization by virtual electron-positron pairs. For the nucleons we see a large difference between the actual values (2.21) and the Dirac values, $g_p^s = 2$, $g_n^s = 0$. This difference (*anomalous* magnetic moments) is generated by strong QCD interactions responsible for the intrinsic structure of the nucleon.

Combining the rotational properties of the tensor operators and their properties with respect to spatial inversion (see Appendix B), we can come to important conclusions concerning multipole moments as physical observables.

The electric charge (2.9) is a scalar invariant under inversion. The electric dipole (2.10) changes sign as the radius vector, or any "normal" (*polar*) vector. The momentum **p** is also a polar vector. However, the orbital angular momentum (A.3) is an *axial* vector; its components do not change sign under inversion. As seen from the geometrical picture of rotation (it does not change sense in the inverted frame), any angular momentum including spin should be an axial vector. The scalar product of an axial vector by a polar vector is a *pseudoscalar*. Similar to scalars, pseudoscalars are invariant under rotations, but change sign under inversion. An important example of a pseudoscalar is given by the *helicity* of a particle,

$$h = \left(s \cdot \frac{\mathbf{p}}{|\mathbf{p}|} \right), \tag{2.22}$$

that is, a spin component along the direction of motion.

Thus, in addition to the tensor properties under transformations from the rotation group, we can classify the operators O by their behavior under spatial inversion $\mathcal{P}$, that is, by their parity $\Pi(O)$, defined by the operator transformation $O' = \mathcal{P}O\mathcal{P} = \pm O$. Acting between the states $|i\rangle$ and $|f\rangle$ with parity Π_i and Π_f, respectively, an operator O has the additional selection rule

$$\Pi_f = \Pi(O)\Pi_i \quad \text{or} \quad \Delta\Pi = \Pi_O. \tag{2.23}$$

Table 2.1 Allowed (+) electromagnetic multipoles for quantal systems with different values of angular momenta. The entries in parentheses are allowed by rotational symmetry but forbidden by parity.

Spin	E0	M0	E1	M1	E2	M2	E3	M3
0	+	−	−	−	−	−	−	−
1/2	+	−	(−)	+	−	−	−	−
1	+	−	(−)	+	+	(−)	−	−
3/2	+	−	(−)	+	+	(−)	(−)	+

It is easy to see that the parity selection rules for electric and magnetic multipoles are complementary (the electric multipoles sometimes are said to have *natural parity*),

$$E\lambda: \quad \Delta\Pi = (-)^{\lambda}, \quad M\lambda: \quad \Delta\Pi = (-)^{\lambda+1}. \tag{2.24}$$

Therefore, the expectation values (diagonal matrix elements, $f = i$) are forbidden for odd electric and even magnetic multipoles if the state has definite parity. In particular, any system in a state of certain parity cannot have a nonzero electric dipole moment.

Table 2.1 summarizes the allowed (+) electromagnetic multipoles for quantal systems with different values of angular momenta (spins). The entries in parentheses are allowed by rotational symmetry but forbidden by parity. The nucleons can have electric charge and magnetic moment; the electric dipole moment can be allowed if parity is not conserved and the stationary states do not have certain parity. Higher multipoles are strictly forbidden by rotational symmetry.

Parity conservation in strong and electromagnetic interactions means that the corresponding Hamiltonian is invariant under inversion (genuine scalar). Then its eigenstates can always be chosen in such a way that they have definite parity. However, this choice is not mandatory. If some states with opposite parities have the same energy (are degenerate), any linear combination of them is also stationary but with no definite parity. For example, the photon circular polarization is its *helicity*. The photon with the left circular polarization has no definite parity. Under inversion this state is transformed into the state with the right circular polarization and the same energy. If the radiation from an unpolarized system contains the left- and right-polarized photons with different probabilities, this means that parity is not conserved in the transition. Similar conclusions may be drawn from experiments with longitudinally (along the momentum) polarized particles.

2.4 Experimental Data for the Deuteron

and the neutron join to form the deuteron, and it should be returned in the form of energy if we want to separate the deuteron again in its constituents. This *binding energy* exists, with different values, for any nucleus; it is in fact a general property imposed by the theory of the relativity to all bound systems.

An indirect method to measure the binding energy of the deuteron is through measurement of its atomic mass, comparing the result with the sum of the masses of the proton and the neutron. Another method, more direct, consists of an experimental measurement of the gamma ray energy emitted when the neutron and the proton combine to form a bound state (n-p capture). One can also measure the inverse process, that is, the energy of the gamma ray necessary to break the binding between the proton and the neutron (photo-disintegration). The first two methods supply the more precise results and one can extract the value for the binding energy of the deuteron,

$$E_B = (2.22464 \pm 0.00005) \text{ MeV.} \tag{2.25}$$

(b) *Angular momentum and parity*. The angular momentum of the deuteron was determined as being $J = 1$, coming from results of optical, radio frequency, and microwave methods.

The parity of a nuclear state cannot be measured directly. It is obtained by analyzing the conservation of parity of certain nuclear disintegrations. Those studies show that a wavefunction with even parity supplies the more appropriate theoretical description for the deuteron.

(c) *Magnetic dipole moment*. The magnetic moment of the deuteron can be obtained as a function of the magnetic moment of the 'proton using the method of magnetic resonance for a molecular beam. This method measures the frequency, or quantum energy, necessary to redirect through 180° the magnetic moment of a nucleus in a periodic magnetic field. The result of the measurements gives the value

$$\mu_d/\mu_p = 0.30701218 \pm 0.00000002. \tag{2.26}$$

That is,

$$\mu_d = (0.857393 \pm 0.000001)\mu_N. \tag{2.27}$$

where $\mu_N = eh/(2m_N c)$ is the nuclear magneton.

(d) *Electric quadrupole moment*. Rabbi and collaborators [Ra33] have shown that the deuteron also has an electric quadrupole moment that makes it look like a prolate spheroid along its spin axis, with the mean square values of the coordinates z and r of the proton obeying the ratio

$$\frac{\langle z^2 \rangle}{\langle r^2 \rangle} = \frac{1.14}{3}. \tag{2.28}$$

instead of $\frac{1}{3}$, as it should be for a spherically symmetric distribution of charge, since $\langle r^2 \rangle = \langle x^2 \rangle + \langle y^2 \rangle + \langle z^2 \rangle$. The quadrupole moment that corresponds to that deformation has the experimental value $Q_d = 0.00282$ barns (1 barn = 10^{-28}m^2).

(e) *The radius of the deuteron*. Hofstadter and collaborators [Ho62] have performed precise measurements of the radius of the proton, deuteron, and complex nuclei, through electron scattering. They obtained the value 2.1 fm for the mean square radius of the deuteron. The same measurement for the proton resulted in the value of 0.8 fm.

2.5 A Square-well Model for the Deuteron

In a quantum description of the deuteron, it is reasonable to suppose that the ground state is an S state that is, a state with zero angular momentum. With $l = 0$, Ψ is spherically symmetric and the angular momentum of the nucleus is entirely due to its spin. As the spins of the proton and neutron are $\frac{1}{2}$, and that of the deuteron is 1, this means that their spins are parallel. In such situation, the magnetic moments would be due to a simple sum:

$$\mu_d \cong \mu_p + \mu_n = 0.8797 \, \mu_N. \tag{2.29}$$

Comparing this result with the value given in (2.27) we see that the difference is 0.0223 μ_N. Therefore, the magnetic moment value of the deuteron almost agrees with the sum of the moments of the proton and of the neutron. The reason for the small difference will be discussed later.

Similarly to that for the hydrogen atom, the Schrödinger equation for the deuteron can be solved reducing the two-body problem to a one-body problem that has the reduced mass of the system and whose distance from the origin is the distance between the two bodies. In the center of mass system of the deuteron, the Schrödinger equation is

$$-\frac{\hbar^2}{2M} \nabla^2 \Psi + V(r)\Psi = E\Psi. \tag{2.30}$$

where

$$M = \frac{M_n M_p}{M_n + M_p} \tag{2.31}$$

is the reduced mass and $V(r)$ is the potential that describes the force between the proton (mass M_p) and the neutron (mass M_n). The difference from the hydrogen atom is that the nuclear potential $V(r)$ is not well known, but, for a first approach, we shall use a very simple form for that potential. We shall suppose initially that V is spherically symmetric, that is, that it depends only on the separation distance between the proton and the neutron, or, $V(\mathbf{r}) = V(r)$. In this case, the wavefunctions Ψ, solutions of (2.30), can be separated into radial and angular parts,

$$\Psi = \sum_{l,m} \frac{u_l(r)}{r} Y_l^m(\theta, \phi). \tag{2.32}$$

where the indexes l and m admit the values

$$l = 0, 1, 2, \ldots, \quad m = -l, -l+1, \ldots, l. \tag{2.33}$$

$Y_l^m(\theta, \phi)$ is the spherical harmonic function (see Appendix A), and u_l the solution of the radial equation

$$\frac{d^2 u_l}{dr^2} + \frac{2M}{\hbar^2}\left[E - V(r) - \frac{l(l+1)}{2Mr^2}\right] u_l = 0. \tag{2.34}$$
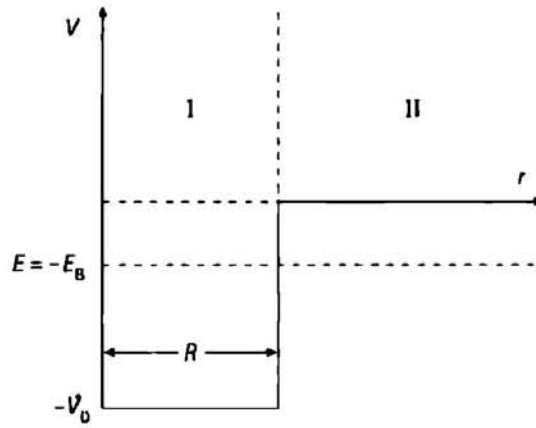
Figure 2.1 Potential well proposed for the deuteron.

The last term inside the brackets is known as the *centrifugal potential*. When $V(r)$ is negative (attractive potential), the centrifugal potential acts to decrease the attraction, making the system less tightly bound. In those circumstances it is easy to see that when $l = 0$ we have a situation where the system is more bound, that is, the energy is the lowest possible; the ground state of a spherically symmetric system is always a state with $l = 0$.

The simplest potential we can imagine for the deuteron is the "tri-dimensional square-well," illustrated in figure 2.1. The radius R and depth V_0 should be adjusted in a way to reproduce the experimental data. In region I, for $l = 0$, we have, omitting the index of u, that

$$\frac{d^2 u}{dr^2} + \frac{2M}{\hbar^2} [V_0 - E_B] u = 0. \tag{2.35}$$

where the well-known experimental fact $E = -E_B = -2.225$ MeV is used, with V_0 and E_B positive numbers. The solution of this equation, which satisfies the boundary condition $u = 0$ at $r = 0$, is

$$u_I = A \sin(Kr), \tag{2.36}$$

where A is a normalization constant and

$$K = \frac{1}{\hbar}\sqrt{2M(V_0 - E_B)}. \tag{2.37}$$

In region II the radial equation assumes the form

$$\frac{d^2 u}{dr^2} - \frac{2M}{\hbar^2} E_B u = 0, \tag{2.38}$$

whose solution, which satisfies the boundary condition $u = 0$ at $r = \infty$, is

$$u_{II} = Be^{-kr}, \tag{2.39}$$

where B is a normalization constant and
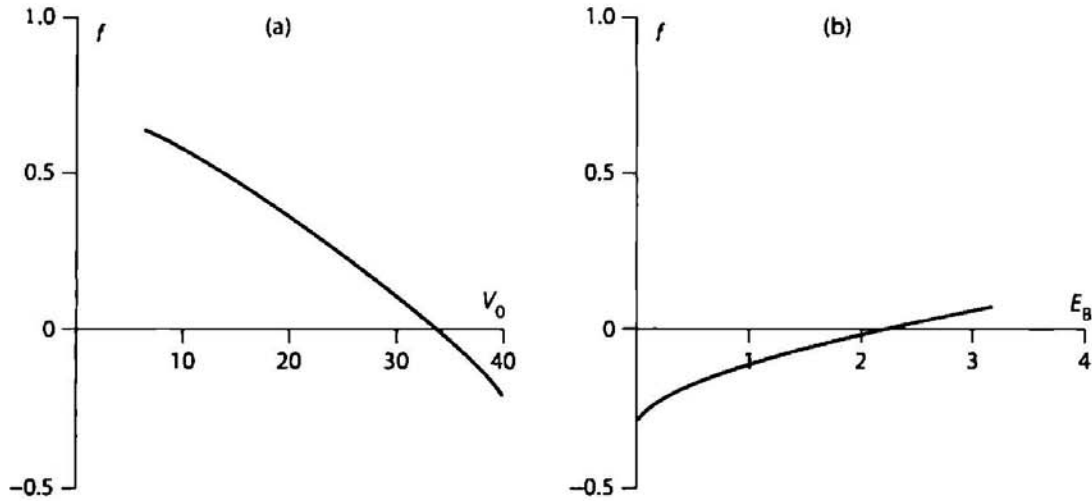
$$k = \frac{1}{\hbar}\sqrt{2ME_B}. \tag{2.40}$$

Figure 2.2 One way of solving an equation like (2.43) is to find graphically the roots of the function $f = K \cot(KR) + k$. In (a) f is plotted as a function of the depth V_0 of the deuteron potential, using $E_B = 2.225$ MeV. The function has a root for $V_0 \cong 34$ MeV. Using this value of V_0 in (b), the same function is plotted against the binding energy E_B, showing that there is no other solution besides the previous one.

The solutions (2.36) and (2.39) should match at $r = R$ so that both the function u and its derivative are continuous at that point. That is also the only way to satisfy the Schrödinger equation at that point. Those conditions imply that

$$AK \cos(KR) = -kBe^{-kR}.\tag{2.41}$$

$$A \sin(KR) = Be^{-kR}.\tag{2.42}$$

Dividing (2.41) by (2.42), we find

$$K \cot(KR) = -k.\tag{2.43}$$

Equation (2.43) implicitly relates the binding energy E_B to the width R and depth V_0 of the potential. As E_B is measured experimentally, (2.43) gives us a relationship between the unknown parameters V_0 and R. If we use $R = 2.1$ fm, the "electromagnetic radius" of the deuteron obtained in the measurement of Hofstadter with electron scattering, (2.43) for V_0 can be solved numerically or graphically (figure 2.2a), yielding a value $V_0 \cong 34$ MeV for the depth of the well for the deuteron. If, inversely, we use the value of V_0 in 2.43 we can see (figure 2.2b) that it does not have a solution for any other value of E_B. We conclude that there are no excited states for $l = 0$. For $l > 0$, the centrifugal potential inhibits even more the formation of a bound state. The nuclear potential would have to be deeper so that the binding is not broken by the centrifugal force.

An important experimental fact is that the total angular momentum of the deuteron is $J = 1$. If the assumption of a $l = 0$ state is correct, it is certain that the intrinsic spin of the deuteron is $S = 1$ (the proton and the neutron with parallel spin vectors). In spectroscopic terminology, this is known as a *triplet state*, denoted by $^3S_1$, where the upper index is the same as $2S + 1$ and the lower index is the value of J. If the nuclear forces were independent

of the spin, we would observe a *singlet state*, $^1S_0$, with the same energy, and that is not the case. In fact, no state with $J = 0$ for the deuteron has been found experimentally, indicating that the neutron-proton force is stronger when the spins are parallel than when they are antiparallel. These forces will be studied in detail later.

2.6 The Deuteron Wavefunction

The fact that the quadrupole moment of the deuteron is different from zero and that the magnetic moment of the deuteron is not the sum of the magnetic moments of the proton and of the neutron indicates that the deuteron cannot have a spherically symmetric wavefunction as in the case of a $^1S_1$ state.

We can discover the nature of the ground state wavefunction of the deuteron using the information that it has a definite parity, and that $J = 1$. The possible states of orbital angular momentum l and spin S are

$$l = 0 \quad S = 1 \quad \rightarrow \quad ^3S_1.$$
$$l = t \quad S = 0 \quad \rightarrow \quad ^1P_1.$$
$$l = 1 \quad S = 1 \quad \rightarrow \quad ^3P_1.$$
$$l = 2 \quad S = 1 \quad \rightarrow \quad ^3D_1.$$

Therefore, the deuteron wavefunction can only be a combination of the $^3S_1$ and $^3D_1$ states (even parity) or a combination of the $^1P_1$ and $^3P_1$ states (odd parity). We should verify which of those combinations represents better the ground state wavefunction of the deuteron with the observed properties.

To build the wavefunction it will be necessary to consider that it is an eigenfunction of the total angular momentum of the system, which is obtained by the addition (coupling) of three vectors, the spins of each nucleon and the orbital angular momentum. At this point it is good to recall how one obtains the wavefunction resulting from the coupling of two angular momenta. For more details, see Appendix B.

2.6.1 Angular momentum coupling

Let us imagine two independent systems, without interaction, where the wavefunctions $|j_1 m_1\rangle$ and $|j_2 m_2\rangle$ describe the behavior of each system, with respective angular momenta j_1 and j_2. In this case,

$$j_1^2 |j_1 m_1\rangle = j_1(j_1 + 1) |j_1 m_1\rangle. \quad j_{1z} |j_1 m_1\rangle = m_1 |j_1 m_1\rangle. \tag{2.44}$$

with identical expressions for the ket 2.[1]

---

[1] Using the Dirac notation, $\Psi^- \equiv \langle\Psi|$ is a *bra* and $\Psi \equiv |\Psi\rangle$ is a *ket*.

Little will change if we include the kets $|j_1 m_1\rangle$ and $|j_2 m_2\rangle$ in a single ket

$$|j_1 j_2 m_1 m_2\rangle \equiv |j_1 m_1\rangle |j_2 m_2\rangle, \tag{2.45}$$

for which the relationships

$$j_1^2 |j_1 j_2 m_1 m_2\rangle = j_1(j_1 + 1) |j_1 j_2 m_1 m_2\rangle, \text{ etc.} \tag{2.46}$$

are valid.

Let us now place the two systems in interaction. j_1 and j_2 will not be constants of motion any more, but will precess around the total angular momentum $j = j_1 + j_2$. The possible values of j will be $|j_1 - j_2|$, $|j_1 - j_2| + 1, \ldots, j_1 + j_2$. The projections m_1 and m_2 will not be good quantum numbers any more, but the projection $m = m_1 + m_2$ will be, so that the wavefunction adequate to the description of the system can be represented by the ket $|j_1 j_2 j m\rangle$.

The wavefunction (2.46) that describes the two joint systems without interaction is no longer valid in the present case. However, it does form a basis in which the wavefunction with interaction can be expanded. Thus,

$$|j_1 j_2 j m\rangle = \sum_{m_1, m_2} \langle j_1 j_2 m_1 m_2 | j m\rangle \, | j_1 j_2 m_1 m_2\rangle \tag{2.47}$$

is the proper expansion, where the sum on m_1 and m_2 reduces to a single sum, if we take in consideration that $m_1 + m_2 = m$. The quantities

$$\langle j_1 j_2 m_1 m_2 | j m\rangle \tag{2.48}$$

are denominated *Clebsh-Gordan coefficients*, and they can be obtained from the algebra of angular momenta. The coefficients are also found in tables where the input data are the six values that appear in (2.48).

2.6.2 Two particles of spin $\frac{1}{2}$

Before proceeding to general theory let us consider a simple important example of two particles of spin $\frac{1}{2}$, $s_1 = s_2 = \frac{1}{2}$. The single-particle spinors χ_m, $m = \pm\frac{1}{2}$, are studied in Appendix A. Two states of each particle give rise to four states $\chi_m(1)\chi_{m'}(2)$ of the representation (B.25). Now we can explicitly proceed along the line sketched in the preceding subsection.

According to our rules, the vector coupling of two spins defines two multiplets, *triplet* and *singlet*, with the values of the total spin $S = s_1 + s_2$ equal to 1 (three states, $S_z = \pm 1, 0$) and 0 (one state $S_z = 0$), respectively. The highest, $M = 1$ and the lowest, $M = -1$, states (B.27) belonging to the triplet are constructed uniquely from the corners of the diagram,

$$\left|\frac{1}{2}, \frac{1}{2}; 1 1\right\rangle = \chi_+(1)\chi_+(2), \quad \left|\frac{1}{2}, \frac{1}{2}; 1 - 1\right\rangle = \chi_-(1)\chi_-(2). \tag{2.49}$$

of (B.34), the triplet combination with $S_z = 0$,

$$|10\rangle = \frac{1}{\sqrt{2}}(\chi_+(1)\chi_-(2) + \chi_-(1)\chi_+(2)).$$ (2.50)

The orthogonal combination with $S_z = 0$, (B.35),

$$|00\rangle = \frac{1}{\sqrt{2}}(\chi_+(1)\chi_-(2) - \chi_-(1)\chi_+(2)).$$ (2.51)

belongs to the singlet $S = 0$.

Note that all three triplet states, (2.49) and (2.50), are *symmetric* with respect to interchange of spins $1 \leftrightarrow 2$, whereas the singlet state (2.51) is *antisymmetric*. We show in Appendix B, in relation to parity and in decomposition of the second rank tensor, that the intrinsic symmetry given by an operation commuting with rotations should be the same for all members of the multiplet. Let the *spin exchange* operator $\mathcal{P}^\sigma$ interchange the spin variables of the pair. Then it can be expressed via the total spin S of the pair,

$$\mathcal{P}^\sigma = (-)^{S-1}.$$ (2.52)

The alternative expression can be derived in terms of the Pauli spin operators (A.82), $\sigma = 2s$. Using

$$(\sigma_1 \cdot \sigma_2) = 4(s_1 \cdot s_2) = 4\frac{S^2 - s_1^2 - s_2^2}{2}.$$ (2.53)

and replacing the angular momentum squares by their eigenvalues, we get

$$(\sigma_1 \cdot \sigma_2) = 2S(S+1) - 3 = \begin{cases} -3 \ (S = 0, \ \text{singlet}), \\ +1 \ (S = 1, \ \text{triplet}). \end{cases}$$ (2.54)

Therefore the exchange operator (2.52) can be written as

$$\mathcal{P}^\sigma = \frac{1 + (\sigma_1 \cdot \sigma_2)}{2}.$$ (2.55)

The spin wavefunctions, $\chi_S^{m_S}$, should now be coupled to the eigenfunctions of orbital angular momentum, Y_l^m, to obtain the angular part $\mathcal{Y}$ of the total wavefunction. Based on (2.47) we can write

$$\mathcal{Y}_{lSJ}^M = \sum_{m_S, m_l} (lSm_lm_S \mid JM)\chi_S^{m_S} Y_l^{m_l}.$$ (2.56)

2.6.3 Total wavefunction

The ground state of the deuteron has $J = 1$. Thus, only the four states calculated below will be considered:

$^3S_1 : J = 1, M = 1, l = 0,$ and $S = 1$

$$\mathcal{Y}^1_{011} = \langle 0101 \mid 11 \rangle Y^0_0 \alpha(1)\alpha(2) = Y^0_0 \alpha(1)\alpha(2);$$ (2.57)

where we define

$$\chi^{+1/2}_{1/2} = \alpha \qquad \text{and} \qquad \chi^{-1/2}_{1/2} = \beta .$$ (2.58)

$^3D_1 : J = 1, M = 1, l = 2,$ and $S = 1$

$$\mathcal{Y}^1_{211} = \sum_{m_S} \langle 21(1 - m_S)m_S \mid 11 \rangle Y^{1-m_S}_2 \chi^{m_S}_1$$

$$= \sqrt{3/5}\, Y^2_2 \beta(1)\beta(2) - \sqrt{3/10}\, Y^1_2 \frac{1}{\sqrt{2}}[\alpha(1)\beta(2) + \beta(1)\alpha(2)]$$

$$+ \sqrt{1/10}\, Y^0_2 \alpha(1)\alpha(2);$$

$^1P_1 : J = 1, M = 1, l = 1,$ and $S = 0$

$$\mathcal{Y}^1_{101} = \langle 1010 \mid 11 \rangle Y^1_1 \chi^0_0 = Y^1_1 \frac{1}{\sqrt{2}}[\alpha(1)\beta(2) - \alpha(2)\beta(1)];$$ (2.59)

$^3P_1 : J = 1, M = 1, l = 1,$ and $S = 1$

$$\mathcal{Y}^1_{111} = \sum_{m_S} \langle 11(1 - m_S)m_S \mid 11 \rangle Y^{1-m_S}_1 \chi^{m_S}_1$$

$$= \frac{1}{\sqrt{2}}\, Y^1_1 \frac{1}{\sqrt{2}}[\alpha(1)\beta(2) + \beta(1)\alpha(2)] - \frac{1}{\sqrt{2}}\, Y^0_1 \alpha(1)\beta(2).$$

For the deuteron, let us make the index 1 in α and β to correspond to the proton and the index 2 to the neutron. We can write the wavefunction $\Psi^M_{lSJ}(\mathbf{r}, \chi)$ for the four cases discussed in terms of the radial wavefunctions $u_l(r)$, where l refers to the orbital angular momentum:

$$^3S_1 : \quad \Psi_S \equiv \Psi^1_{011} = \frac{u_0(r)}{r} \mathcal{Y}^1_{011} = \frac{u_0(r)}{r} Y^0_0 \chi^1_1;$$ (2.60)

$$^3D_1 : \quad \Psi_D \equiv \Psi^1_{211} = \frac{u_2(r)}{r} \mathcal{Y}^1_{211} = \frac{u_2(r)}{r} \left[\sqrt{\frac{3}{5}}\, Y^2_2 \chi^{-1}_1 - \sqrt{\frac{3}{10}}\, Y^1_2 \chi^0_1 + \sqrt{\frac{1}{10}}\, Y^0_2 \chi^1_1 \right];$$ (2.61)

$$^1P_1 : \quad \Psi_{1P} \equiv \Psi^1_{101} = \frac{u_1(r)}{r} \mathcal{Y}^1_{101} = \frac{u_1(r)}{r} Y^1_1 \chi^0_0;$$ (2.62)

$$^3P_1 : \quad \Psi_{3P} \equiv \Psi^1_{111} = \frac{u_1(r)}{r} \mathcal{Y}^1_{111} = \frac{u_1(r)}{r} \left[\frac{1}{\sqrt{2}}\, Y^1_1 \chi^0_1 - \frac{1}{\sqrt{2}}\, Y^0_1 \chi^1_1 \right].$$ (2.63)

Noticing that in the center of mass system the orbital angular momentum associated to the proton is half of the relative orbital momentum, $l_p = \frac{1}{2}l$, gives z-component of the magnetic moment of the deuteron:

$$\mu_z = \frac{1}{2}l_z + g_p S^z_p + g_n S^z_n,$$ (2.64)

in units of μ_N, the nuclear magneton, with $g_p = 5.58$ and $g_n = -3.82$.

The magnetic moment of the deuteron is defined as

$$\mu = \left\langle \Psi^J_{lSJ} \,|\mu_z|\, \Psi^J_{lSJ} \right\rangle = \left\langle \frac{u_l}{r} \mathcal{Y}^J_{lSJ} \,\Big|\mu_z\Big|\, \frac{u_l}{r} \mathcal{Y}^J_{lSJ} \right\rangle. \tag{2.65}$$

If we take into consideration that (in units of $\hbar$)

$$l_z Y^m_l = m Y^m_l. \tag{2.66}$$

and that

$$S^z_p \chi^1_1 = \frac{1}{2} \chi^1_1, \qquad\qquad S^z_n \chi^1_1 = \frac{1}{2} \chi^1_1,$$

$$S^z_p \chi^0_1 = \frac{1}{2} \chi^0_0, \qquad\qquad S^z_n \chi^0_1 = -\frac{1}{2} \chi^0_0,$$

$$S^z_p \chi^{-1}_1 = -\frac{1}{2} \chi^{-1}_1, \qquad\qquad S^z_n \chi^{-1}_1 = -\frac{1}{2} \chi^{-1}_1,$$

$$S^z_p \chi^0_0 = \frac{1}{2} \chi^0_1, \qquad\qquad S^z_n \chi^0_0 = -\frac{1}{2} \chi^0_1.$$

we obtain

$$\mu_z \mathcal{Y}^1_{011} = \frac{1}{2}(g_p + g_n)\mathcal{Y}^1_{011} = \frac{1}{2}(g_p + g_n) Y^0_0 \chi^1_1; \tag{2.67}$$

$$\mu_z \mathcal{Y}^1_{211} = \sqrt{\frac{3}{5}}\left(1 - \frac{g_p + g_n}{2}\right) Y^2_2 \chi^{-1}_1 - \frac{1}{2}\sqrt{\frac{3}{10}} Y^1_2 [\chi^0_1 + (g_p - g_n)\chi^0_0] + \sqrt{\frac{1}{10}} \frac{g_p + g_n}{2} Y^0_2 \chi^1_1; \tag{2.68}$$

$$\mu_z \mathcal{Y}^1_{101} = \frac{1}{2} Y^1_1 [\chi^0_0 + (g_p - g_n)\chi^0_1]; \tag{2.69}$$

$$\mu_z \mathcal{Y}^1_{111} = \frac{1}{2\sqrt{2}} [Y^1_1 \chi^0_1 + g_p(Y^1_1 \chi^0_0 - Y^0_1 \chi^1_1) - g_n(Y^1_1 \chi^0_0 + Y^0_1 \chi^1_1)]. \tag{2.70}$$

Using the orthonormality of Y^m_l and of the $\chi^{m_s}_S$, we obtain the expected values

$$^3S_1 : \langle \Psi^1_{011} \,|\, \mu_z \,|\, \Psi^1_{011} \rangle = \frac{g_p + g_n}{2} \int_0^\infty u^2_0(r)\, dr = \frac{g_p + g_n}{2} = 0.88 \mu_N; \tag{2.71}$$

$$^3D_1 : \langle \Psi^1_{211} \,|\, \mu_z \,|\, \Psi^1_{211} \rangle = \left[\frac{3}{4} - \frac{1}{4}(g_p + g_n)\right] \int_0^\infty u^2_2(r)\, dr$$

$$= \frac{3}{4} - \frac{1}{4}(g_p + g_n) = 0.31 \mu_N; \tag{2.72}$$

$$^1P_1 : \langle \Psi^1_{101} \,|\, \mu_z \,|\, \Psi^1_{101} \rangle = \frac{1}{2} \int_0^\infty u^2_1(r)\, dr = 0.5 \mu_N; \tag{2.73}$$

$$^3P_1 : \langle \Psi^1_{111} \,|\, \mu_z \,|\, \Psi^1_{111} \rangle = \left[\frac{1}{4} + \frac{1}{4}(g_p + g_n)\right] \int_0^\infty u^2_1(r)\, dr$$

$$= \frac{1}{4} + \frac{1}{4}(g_p + g_n) = 0.69 \mu_N. \tag{2.74}$$

The experimental value of the magnetic moment of the deuteron is $0.8573\ \mu_N$, different from all values found above. Thus, the deuteron cannot be found exclusively in any of the states mentioned previously. In order for the magnetic moment to be equal to the

experimental value, one is forced to conclude that the ground state of the deuteron should be a mixture of these states. Therefore, we construct the possible mixtures of states of same parity,

$$\Psi = C_S \Psi_S + C_D \Psi_D \tag{2.75}$$

or

$$\Psi = C_{1p} \Psi_{1p} + C_{1p} \Psi_{1p}. \tag{2.76}$$

and the normalization condition $\langle \Psi \mid \Psi \rangle = 1$ gives

$$C_S^2 + C_D^2 = 1 \tag{2.77}$$

or

$$C_{1p}^2 + C_{1p}^2 = 1. \tag{2.78}$$

From (2.71), (2.72), and (2.75) we find

$$\langle \Psi \mid \mu_z \mid \Psi \rangle \frac{1}{2}(g_p + g_n)C_S^2 + \left[\frac{3}{4} - \frac{1}{4}(g_p + g_n)\right]C_D^2 = (0.88C_S^2 + 0.31C_D^2)\mu_N. \tag{2.79}$$

If we make $\langle \Psi \mid \mu_z \mid \Psi \rangle$ equal to the experimental value $0.85573\,\mu_N$, we obtain $C_S^2 = 0.96$ and $C_D^2 = 0.04$. On the other hand, a mixture of $^1P_1$ and $^3P_1$ states cannot take us to the experimental value of μ since in both states the magnetic moment is smaller than μ_d. We should conclude that the ground state of the deuteron is basically (96%) a $^3S_1$ state, with a small (4%) contribution of the $^3D_1$ state. Therefore, the wavefunction of the deuteron can be written as

$$\Psi_d = C_S \frac{u_0}{r} \mathcal{Y}_{011}^1 + C_D \frac{u_2}{r} \mathcal{Y}_{211}^1. \tag{2.80}$$

Identical results can be obtained by analysis of the electric quadrupole moment.

2.7 Particles in the Continuum: Scattering

When a wave of any type hits a small obstacle, secondary waves (circular or spherical) are produced and move away from it, going to infinity. In the same way, a monoenergetic beam of particles, which can be represented by a plane wave, undergoes scattering when it finds a region in which there exists a potential $V(r)$ created by a nucleus (figure 2.3). Unlike the quantum bound state problem, where one searches for the possible values of the energy of the system, the solution of scattering problems consists in finding the angular distribution of the scattered particles, where the total energy of the system target+projectile can have any positive value.

The angular distribution is determined by the probability of finding the scattered particles as a function of the scattering direction, and this probability is directly connected to the wavefunctions. Thus, given an incident plane wave, whose stationary part can be represented by

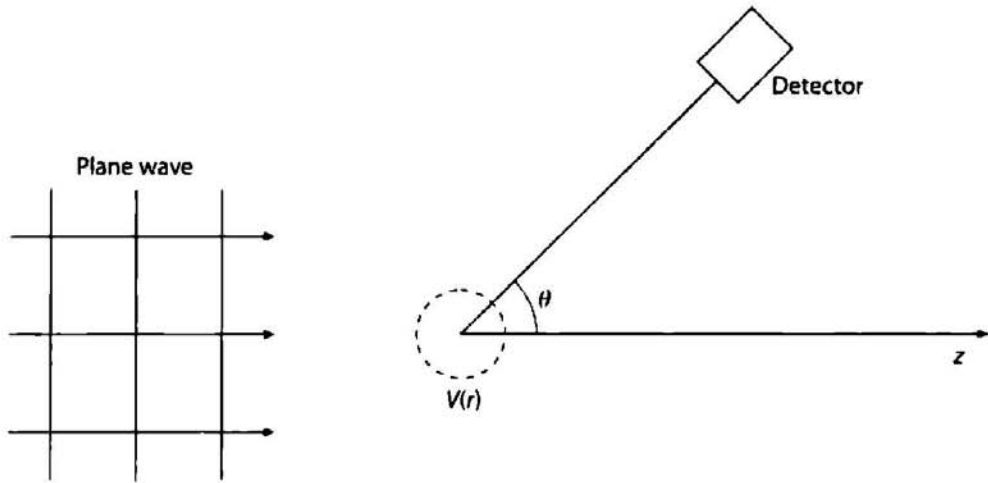$$\Psi i(r) = e^{ik \cdot r} = e^{ikz}, \tag{2.81}$$

Figure 2.3 Scattering of a plane wave by a potential $V(r)$ limited to a small region of space.

and a scattering potential $V(r)$, our problem reduces to finding the wavefunction of the scattered particles, or the scattered wavefunction.

In problems of atomic and nuclear physics the detectors lie far away from the scattering centers compared to their dimensions, that is, they are in a region where the particles no longer feel the action of the potential. Thus, our interest will be limited to the asymptotic part of the scattered wavefunction, namely, its form when $r \to \infty$. When a short range potential $V(r)$, supposed for simplicity to be spherically symmetric, acts on the particles of an incident beam, a detector placed in the asymptotic region will register not only the presence of the plane wave but also the particles scattered by the potential. That is, to the plane wave will be added an outgoing spherical wave created by the scattering center, and we can write the wavefunction far from this center as

$$\Psi \sim e^{ikz} + f(\theta) \frac{e^{ikr}}{r}. \tag{2.82}$$

where the symbol $\sim$ means asymptotic value. The presence of the function $f(\theta)$ expresses the fact that the scattering directions do not have not the same probability. This function is called *scattering amplitude* and has, as we will see next, an essential role in the theory for the process.

The probability current,

$$j = \frac{h}{m} \operatorname{Im}(\Psi^* \nabla \Psi), \tag{2.83}$$

will be now employed in the definition of a function that measures the angular distribution of the particles scattered by $V(r)$. The current for the incident plane wave is

$$j_i = \frac{h}{m} \operatorname{Im}\left(e^{-ikz} \frac{d}{dz} e^{ikz}\right) = \frac{hk}{m} = v. \tag{2.84}$$

and for the outgoing spherical wave

$$j_r \sim \frac{h}{m} \operatorname{Im}\left\{ f^*(\theta) \frac{e^{-ikr}}{r} \frac{\partial}{\partial r} \left[f(\theta) \frac{e^{ikr}}{r} \right] \right\} = \frac{v}{r^2} |f(\theta)|^2. \tag{2.85}$$
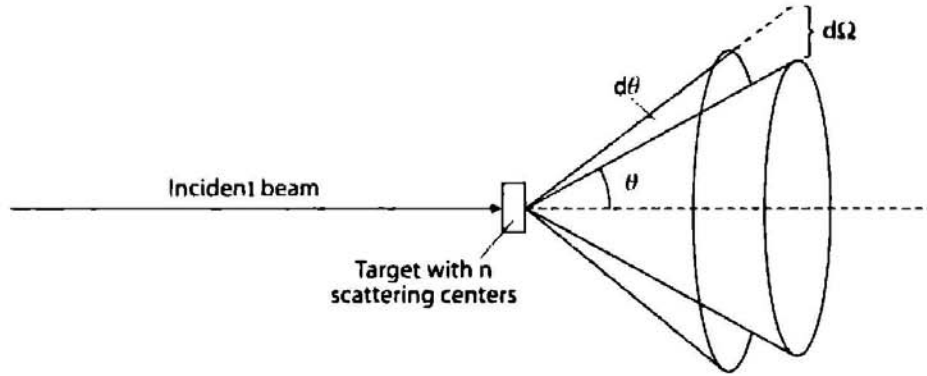
Figure 2.4 Quantities used in the definition of the differential cross section.

We define the *differential cross section*, a function of the angle θ (see figure 2.4), by

$$\frac{d\sigma}{d\Omega} = \frac{dN/d\Omega}{n\Phi}. \tag{2.86}$$

dN being the number of observed events in $d\Omega$ per unit time, n the number of target scattering centers comprised by the beam, and Φ the incident flux (number of incident particles per unit area and per unit time). $d\Omega = 2\pi \sin\theta \, d\theta$ is the solid angle located between the cones defined by the directions θ and $\theta + d\theta$. If our assumption of spherical symmetry for the scatter potential is not valid, the solid angle is the one defined by the direction θ, ϕ, namely, $d\Omega = \sin\theta d\theta d\phi$.

Definition (2.86) is a general one, and the *observed events*, in the present case, are particles scattered by the potential $V(r)$. $d\sigma/d\Omega$ has the dimension of area, and its value is obtained from

$$\frac{d\sigma}{d\Omega} = \frac{j_r r^2}{j_i} \tag{2.87}$$

by the fact that the number of particles that cross a given area per unit time is measured by the probability current flux through that area. With (2.84) and (2.85) it is clear that

$$\frac{d\sigma}{d\Omega} = |f(\theta)|^2. \tag{2.88}$$

being thus the determination of the angular distribution reduced to the evaluation of the scattering amplitude $f(\theta)$.

The *total cross section* is obtained by integrating (2.88):

$$\sigma = \int \frac{d\sigma}{d\Omega} d\Omega = 2\pi \int_{-1}^{+1} |f(\theta)|^2 \, d(\cos\theta), \tag{2.89}$$

and its meaning is obvious from (2.86): the total cross section measures the number of events per target nucleus per unit time divided by the incident flux defined above. It must include, in this way, events for which we cannot define a differential cross section, such as the absorption of particles from the incident beam by the nucleus.

2.8 Partial Wave Expansion

When we study interactions governed by a central potential $V(r)$, solutions of the Schrödinger equation

$$\nabla^2 \Psi + \frac{2m}{\hbar^2} \left[E - V(r) \right] \Psi = 0 \tag{2.90}$$

can be written as linear combinations of products of solutions separated into radial and angular parts:

$$\Psi = \sum_{l,m} a_{lm} \frac{u_l(r)}{r} Y_l^m(\theta, \phi). \tag{2.91}$$

where $u_l(r)$ obeys the radial equation

$$\frac{d^2 u}{dr^2} + \frac{2m}{\hbar^2} \left[E - V(r) - \frac{\hbar^2}{2m} \frac{l(l+1)}{r^2} \right] u = 0 \tag{2.92}$$

and the boundary condition

$$u_l(0) = 0. \tag{2.93}$$

The axial symmetry of our problem allows to eliminate the dependence in ϕ of (2.91) so that

$$\Psi = \sum_l a_l P_l(\cos\theta) \frac{u_l(r)}{kr}. \tag{2.94}$$

where the constant $k = \sqrt{2mE}/\hbar$ was introduced to make easier later applications of the expansion.

The terms of (2.94) can be understood as *partial waves* from which the general solution Ψ can be constructed. An expression like (2.94) is convenient: if $V(r)$ is spherically symmetric, the angular momentum is a constant of motion, and states of different values of the angular momentum contribute in an independent way to the scattering. Thus, it is also useful to present the plane wave by an expansion in Legendre polynomials

$$e^{ikz} = e^{ikr\cos\theta} = \sum_{l=0}^{\infty} (2l+1) i^l j_l(kr) P_l(\cos\theta), \tag{2.95}$$

where $j_l(x)$ are spherical Bessel functions and $P_l(\cos\theta)$ the Legendre polynomials.

Expression (2.95) has the form of (2.94). This means that the plane wave $e^{i\mathbf{k}\cdot\mathbf{r}}$ can be understood as the sum of a set of partial waves, each one with orbital angular momentum $\sqrt{l(l+1)}\,\hbar$. The terms $j_l(kr) P_l(\cos\theta)$ specify the radial and angular dependence of the partial wave l, the weight of the contribution of each term being given by the amplitude $2l+1$ and the phase factor i^l.

Using classical arguments we can give an interpretation to this amplitude value. Let us consider a surface normal to the plane wave propagation direction, and imagine a set of circles of radius $b_l = l\bar{\lambda}$, with the wavelength $\bar{\lambda} = \lambda/2\pi = 1/k$, centered at the point where the z-axis crosses the surface (see figure 2.5). If the beam of particles moves along
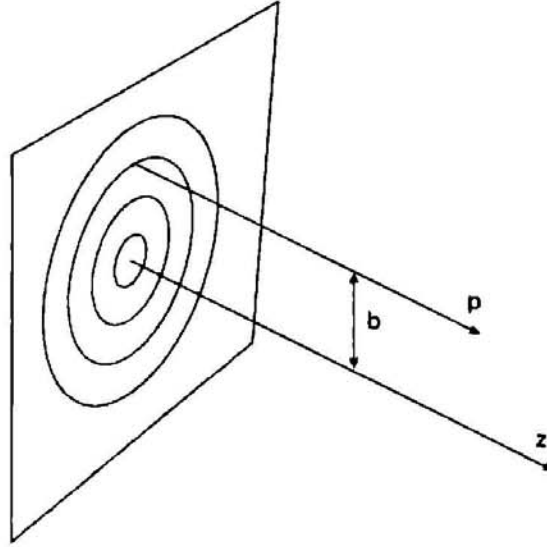
Figure 2.5 Classical representation of a plane wave: to each partial wave *l* corresponds an impact parameter *b*.

the z-axis, the classical angular momentum of a particle about the origin of the coordinate system is the product of the impact parameter *b* and the linear momentum $p = \hbar k$. Hence, all particles that pass by a ring of internal radius b_l and external radius b_{l+1} will have orbital angular momentum between $l\bar{\lambda}\hbar k = l\hbar$ and $(l + 1)\bar{\lambda}\hbar k = (l + 1)\hbar$. In the classical limit *l* is large and $l + 1 \cong l$. So we can say that all the particles that pass through the ring have orbital angular momentum $l\hbar$. However, still using classical reasoning, a particle belonging to a uniform beam can have any impact parameter, and its probability of passing one of the rings is proportional to the area *A* of that ring:

$$A = \pi(b_{l+1}^2 - b_l^2) = \pi\bar{\lambda}^2\left[(l + 1)^2 - l^2\right] = \pi\bar{\lambda}^2(2l + 1). \tag{2.96}$$

We see that $2l + 1$ is the relative probability that a particle in a uniform beam has an orbital angular momentum $l\hbar$, which is the classical limit for the orbital angular momentum $\sqrt{l(l + 1)}$ associated to the partial wave *l*.

At large distances from the origin the spherical Bessel functions reduce to the simple expression

$$j_l(kr) \sim \frac{\sin\left(kr - \frac{l\pi}{2}\right)}{kr} = \frac{e^{i(kr - \frac{l\pi}{2})} - e^{-i(kr - \frac{l\pi}{2})}}{2ikr}. \tag{2.97}$$

Using (2.97) in (2.95) results in

$$e^{ikr\cos\theta} \sim \frac{1}{2i}\sum_{l=0}^{\infty}(2l + 1)i^l P_l(\cos\theta)\left[\frac{e^{i(kr - \frac{l\pi}{2})} - e^{-i(kr - \frac{l\pi}{2})}}{kr}\right]. \tag{2.98}$$

which represents the asymptotic form of a plane wave.

In (2.98) the first term in the brackets corresponds to an outgoing spherical wave and the second to an incoming spherical wave. Thus, each partial wave in (2.98) is, at large distances from the origin, a superposition of two spherical waves, namely, the incoming and the outgoing components. The total radial flux for the wavefunction $\Psi_i = e^{ikr\cos\theta}$ vanishes,

since the number of free particles that enter a region is the same as the number that exit. This can be easily shown using (2.98) in (2.83) (exercise 9 proposes this demonstration for the more general expression 2.99).

Let us now understand Ψ in (2.94) as a solution of a scattering problem, the scattering being caused by a potential $V(r)$. The asymptotic form of Ψ can be obtained if we observe that the presence of the potential has the effect of causing a perturbation in the outgoing part of the plane wave, and such a perturbation can be represented by a unitary module function, $S_l(k)$.

From (2.98), this leads to

$$\Psi \sim \frac{1}{2i} \sum_{l=0}^{\infty} (2l + 1) i^l P_l(\cos\theta) \frac{S_l(k) e^{i(kr - \frac{l\pi}{2})} - e^{-i(kr - \frac{l\pi}{2})}}{kr}, \tag{2.99}$$

where the function $S_l(k)$ can be represented by

$$S_l(k) = e^{2i\delta_l}. \tag{2.100}$$

When we write the form (2.100) we admit that the scattering is elastic. The unitary module of $S_l(k)$ keeps the same value for the probability current and does not allow that the presence of the potential removes or add particles to the elastic channel k. From a comparison of (2.99) and (2.94) we can obtain the expressions for a_l and for the asymptotic form of $u_l(r)$:

$$a_l = i^l (2l + 1) e^{i\delta_l} \tag{2.101}$$

and

$$u_l(r) \sim \sin\left(kr - \frac{l\pi}{2} + \delta_l\right). \tag{2.102}$$

$u_l(r)$ differs from the asymptotic form of the radial function of a free particle by the presence of the *phase shifts* δ_l; the presence of the scattering potential creates in each partial wave a phase shift δ_l, and the scattering problem would be solved with the determination of these phase shifts for a given potential $V(r)$. In fact, the use of (2.99) and (2.98) in (2.82) results in

$$f(\theta) = \frac{1}{k} \sum_{l=0}^{\infty} (2l + 1) e^{i\delta_l} \sin\delta_l P_l(\cos\theta). \tag{2.103}$$

and the differential cross section (2.88) is obtained from the knowledge of the phase shifts δ_l.

The phase shifts are evaluated by solving (2.92) for each l and comparing the phase of $u_l(r)$, for some large r, with the phase of $j_l(kr)$ for the same value of r. This is depicted in figure 2.6, for a generic value of l and three different situations of the potential $V(r)$.

The first curve shows $u_l(r)$ for the case in which $V(r) = 0$ for all r. In this case, $u_l(r) = j_l(kr)$ and we do not have phase shifts for any l. The middle curve shows $u_l(r)$ when one introduces a small attractive potential acting inside a certain radius r_0, that is, $V(r) < 0$ for $r < r_0$, and $V(r) = 0$ for $r > r_0$. From (2.92) we see that, with this attractive potential, $|E - V(r)| > E$ in the potential region and the quantity d^2u_l/dr^2 will be greater in that
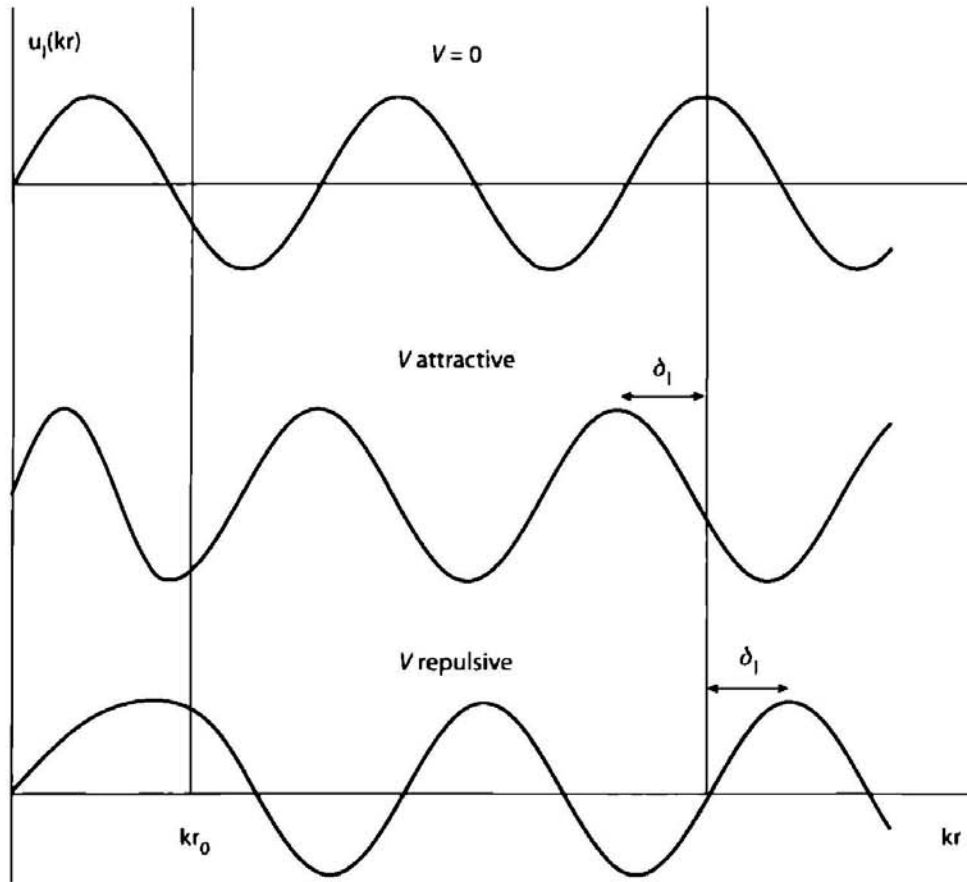
Figure 2.6 Radial part of the wavefunction for three different potentials, showing how the phase shift sign is determined by the function behavior in the region $r < r_0$ where the potential acts.

region than in the region of zero potential. Thus, $u_l(r)$ will oscillate rapidly for $r < r_0$. For $r > r_0$, the behavior is the same as that in the case $V(r) = 0$, except that the phase is displaced. In this way we see that with a small attractive potential, $u_l(r)$ is "pulled in," which in turn advances its phase and makes the phase shift positive. The last curve shows $u_l(r)$ for the case of a small repulsive potential, that is, $V(r) > 0$ for $r < r_0$, and $V(r) = 0$ for $r > r_0$. In this case, $| E - V(r) | < E$ in the potential region and the quantity $d^2 u_l/dr^2$ will be smaller in that region than in the region of zero potential. The result is that, for a repulsive potential, $u_l(r)$ is "pulled out," its phase is retarded, and the phase shift is negative.

The total cross section, in turn, has the expression

$$\sigma = \frac{4\pi}{k^2} \sum_l (2l + 1) \sin^2 \delta_l. \tag{2.104}$$

obtained by the integration (2.89).

From (2.103) and (2.104) one extracts an important relation. For this, it is enough to observe in (2.103) that

$$\text{Im } f(0) = \frac{1}{k} \sum_{l=0}^{\infty} (2l + 1) \sin^2 \delta_l \tag{2.105}$$

and to compare this result with (2.104) to obtain

$$\sigma = \frac{4\pi}{k} \, \mathrm{Im} \, f(0). \tag{2.106}$$

This relation is known as the *optical theorem*. It connects the total cross section with the scattering amplitude at angle zero. This is physically understandable: the cross section measures the removal of particles from the incident beam that arises, in turn, from the destructive interference between the incident and scattered beams at zero angle [Sc54]. We will see in chapter 10 that the optical theorem is not restricted to elastic scattering, being also valid for inelastic processes.

In the sum (2.104) each angular momentum contributes at most a cross section

$$(\sigma)_{\text{max}} = \frac{4\pi}{k^2}(2l + 1). \tag{2.107}$$

a value of the same order of magnitude as the maximum classical cross section per unit $\hbar$ of angular momentum. Actually, if we use the estimate $b = l/k$ for the impact parameter, the contribution of an interval $\Delta l = 1$, or $\Delta b = 1/k$, for the total cross section will be

$$\sigma_l = 2\pi \, b \, \Delta b = 2\pi \, \frac{l}{k^2}. \tag{2.108}$$

For large l this agrees with $(\sigma)_{\text{max}}$, except for a factor 4. The difference is due to the unavoidable presence of diffraction effects for which the wave nature of matter is responsible.

The partial wave analysis (2.103) gives an exact procedure to solve the scattering problem at all energies. For a given potential $V(r)$, (2.92) should be solved and its asymptotic solutions (2.102) used to find the phase shifts δ_l. The infinite number of terms of (2.103) is not a problem in practice, since

$$\lim_{l \to \infty} \delta_l = 0. \tag{2.109}$$

This result can be verified by examining (2.92): for large l the centrifugal potential term, proportional to $l(l + 1)$, is totally dominant, making irrelevant the phase shifts generated by $V(r)$. However, at high energies the sum (2.103) will have the contribution of many terms, since, in this case, $kr_0 \gg 1$, and for all l up to $l_{\text{max}} \simeq kr_0$ there will be appreciable phase shifts. The partial wave analysis is of great utility, especially in the low energy case, which will be treated in the next section.

2.9 Low Energy Scattering

We have seen that the partial wave expansion is useful only at low energies since in this case the number of terms of (2.103) that we have to deal with is small. If the energy is low

enough, the sum (2.103) reduces to the term with $l = 0$. We have, in this case,

$$f(\theta) = \frac{1}{k} e^{i\delta_0} \sin \delta_0 \qquad (2.110)$$

and

$$\sigma = \frac{4\pi}{k^2} \sin^2 \delta_0. \qquad (2.111)$$

The differential cross section that results from (2.110) is independent of θ: the scattering is isotropic. This is easily understandable since at low energies the incident particle wavelength is much greater than the dimension of the target nucleus; during its passage all points in the nucleus are with the same phase at each time, and it is impossible to identify the direction of incidence.

In the extreme case $E \to 0$ the scattering amplitude (2.110) remains finite only if $\delta_0 \to 0$ together with the energy. In this case the phase difference is no more the main scattering parameter. A better parameter is the *scattering length a*, defined as the limit

$$\lim_{E \to 0} f(\theta) = \lim_{k \to 0} \frac{\delta_0}{k} = -a, \qquad (2.112)$$

yielding the equation

$$\sigma = 4\pi a^2 \qquad (2.113)$$

as the expression for the total cross section at the zero energy limit.

The physical meaning of the scattering length can be obtained observing that for $l = 0$, and in the limit $E \to 0$, (2.92) in the region outside the potential reduces to its first term. Hence, if $d^2 u/dr^2 = 0$, we see that the wavefunction u tends to a straight line and the abscissa at the point where this line crosses the r-axis is the scattering length a. This can be easily seen if we rewrite (2.102) in the limit $E \to 0$:

$$u_0(r) \cong kr + \delta_0 = k(r - a). \qquad (2.114)$$

This property will be used later to determine if a state of the system is or not bound.

As an application let us evaluate the cross section of scattering of low energy neutrons by protons. The attractive nuclear potential between a proton and a neutron is put in the simple form

$$V(r) = \begin{cases} -V_0, & \text{if } r < r_0, \\ 0, & \text{if } r < r_0. \end{cases} \qquad (2.115)$$

where r_0 represents the range of the nuclear force. We know that this problem can be reduced to a single particle problem. a particle carrying the reduced mass of the system and subject to the same potential V_0. E turns to be the total system energy in the center of mass frame. For a neutron with energy E_n incident on a proton at rest in the laboratory, E is very close to $E_n/2$.

If $l = 0$ is the only partial wave to contribute, (2.92) assumes the form

$$\frac{d^2u}{dr^2} + \frac{2m}{\hbar^2}(E + V_0)u = 0 \quad (r < r_0).$$ (2.116)

$$\frac{d^2u}{dr^2} + \frac{2m}{\hbar^2}Eu = 0 \quad (r > r_0),$$ (2.117)

with the boundary conditions $u = 0$ in $r = 0$ and u and du/dr continuous at $r = r_0$. From this results

$$u = A \sin(Kr) \quad (r < r_0),$$ (2.118)

with

$$K = \frac{\sqrt{2m(E + V_0)}}{\hbar}.$$ (2.119)

and

$$u = \sin(kr + \delta_0) \quad (r > r_0),$$ (2.120)

where

$$k = \frac{\sqrt{2mE}}{\hbar}.$$ (2.121)

Note that both solutions are of sinusoidal type because $E > 0$. The continuities of the function and its derivative at $r = r_0$ can be expressed by the continuity of $(du/dr)/u$:

$$K \cot(Kr_0) = k \cot(kr_0 + \delta_0)$$ (2.122)

or

$$k \tan(Kr_0) = K \tan(kr_0 + \delta_0),$$ (2.123)

which in the limit $k \to 0$ gives

$$\delta_0 \approx kr_0 \left[\frac{\tan(K_0 r_0)}{K_0 r_0} - 1 \right].$$ (2.124)

where $K_0 = \sqrt{2mV_0}/\hbar$. The total cross section calculated from (2.124) using (2.111) shows singularities at the points where $K_0 r_0$ have values $\pi/2, 3\pi/2$, etc., since the tangent in the numerator of (2.124) makes the cross section diverge. This corresponds physically to the appearance of a bound state at that depth. As we are dealing with very small E, there is a resonance whenever an increase in the well depth gives rise to a new level at zero energy. But, in fact, (2.124) is not valid for the $K_0 r_0$ values above, which violates the approximation from which it was deduced. The exact equation (2.123) shows that, when $Kr_0 = \pi/2, 3\pi/2$, etc., the phase shift is $\delta_0 = Kr_0$, and from (2.111) we see that, for these values of δ_0, the cross section has very large but finite values, given by

$$\sigma = \frac{4\pi}{k^2}.$$ (2.125)

Note that (2.125) can be written as $\sigma = [4/(kr_0)^2] \pi r_0^2$. Since $kr_0 \ll 1$, σ is much greater than πr_0^2, which is the geometrical cross section of the scattering potential. When σ has its maximum possible value for an s-wave scattering, one says that the cross section is in an
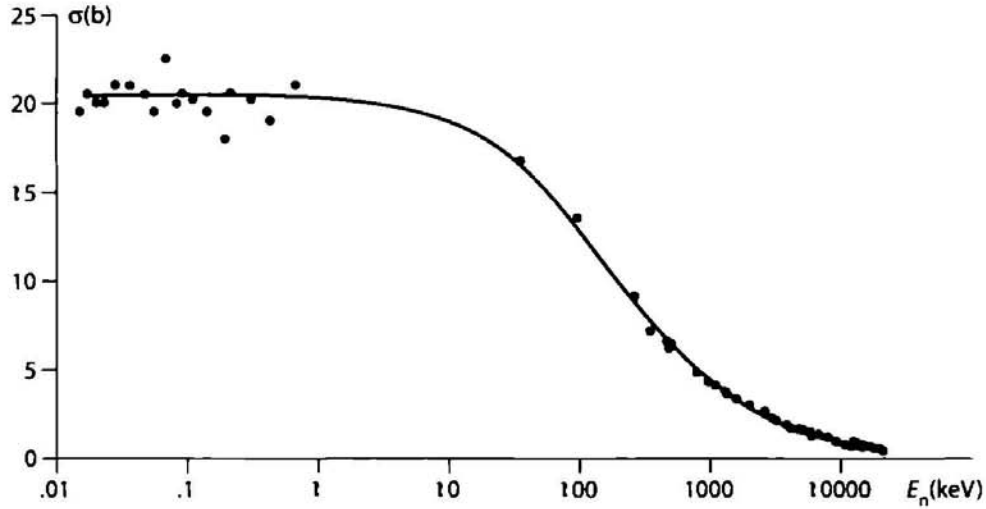
Figure 2.7 Neutron-proton cross sections at low energies. E_n is the energy of the incident neutron. The experimental points were obtained from [Ad50] and [Ho71]. The curve was calculated using (2.144).

s-wave resonance. Resonances in other partial waves occur if E is large enough to create large phase shifts for $l > 0$. For example, when $\delta_1 = \pi/2, 3\pi/2$, etc., the cross section is especially large and one says that we have a p-wave resonance.

Another interesting fact to see in (2.124) is that, if $\tan(K_0 r_0) = K_0 r_0$, the phase shift and the scattering cross section vanish. Hence, for certain values of the well depth there will be no s-wave scattering. This is known as the *Ramsauer effect*, owing to the discovery by C. Ramsauer, in 1921, that the effective cross section for electron scattering in inert gas atoms is very low at energies close to 0.7 eV. The quantum theory gives a simple explanation of this effect, which cannot be explained by the classical theory. The atomic field of inert gases decreases faster with distance than the fields of other atoms; as a first approximation, we can replace this field by a rectangular well and use (2.111) and (2.124) to evaluate the cross section of the low energy electrons. For an electron energy of approximately 0.7 eV, we get $\sigma \sim 0$, if we use r_0 equal to the atomic dimensions.

Let us make an estimate of the neutron-proton cross section. Let us use $V_0 = 34$ MeV for the approximate depth of the deuteron potential. We have

$$K_0 = \frac{\sqrt{2mV_0}}{\hbar} = \frac{\sqrt{2mc^2 V_0}}{\hbar c} = \frac{\sqrt{938.93 \times 34}}{197.33} = 0.91 \text{ fm}^{-1}, \tag{2.126}$$

where m is the reduced mass, equal to half a nucleon mass. Still using $r_0 \cong 2.1$ fm as the deuteron radius, we have

$$a = -\frac{\delta_0}{k} = r_0 \left[1 - \frac{\tan(K_0 r_0)}{K_0 r_0}\right] = 2.1 \times 10^{-13}\left[1 - \frac{\tan(0.91 \times 2.1)}{0.91 \times 2.1}\right] = 5.2 \times 10^{-13} \text{ cm}. \tag{2.127}$$

Hence,

$$\sigma = 4\pi(5.2 \times 10^{-13})^2 \text{cm}^2 \cong 3.5 \text{ b}. \tag{2.128}$$

Figure 2.7 shows experimental values of the neutron-proton cross sections up to 20 MeV. In the zero energy limit the cross section has the value $\sigma = (20.43 \pm 0.02)$ b, six times
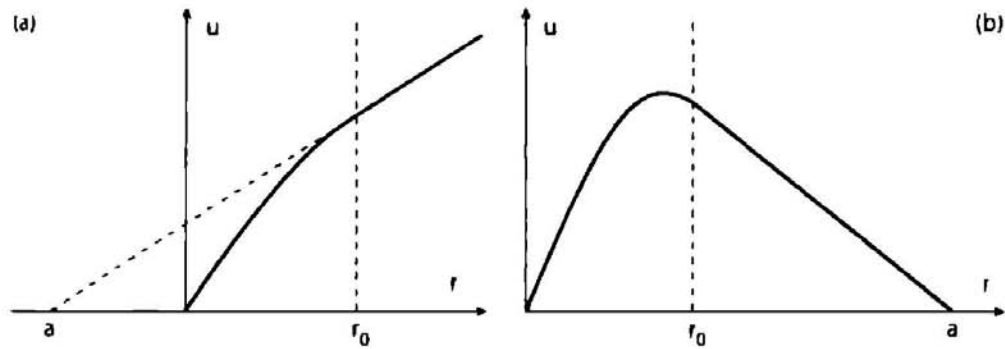
Figure 2.8 Radial part of the scattering wavefunction u at zero energy for two values of the well depth. In (a) the depth is not large enough for the existence of a bound state and the scattering length is negative. In (b) one sees the existence of a bound state, the function u has a maximum inside the potential range and u has a positive value.

greater than the value obtained in (2.128). The reason for this discrepancy was explained by Wigner, proposing that the nuclear force depends on the spin, being different when nucleons collide with parallel (triplet) spins or with antiparallel spins (singlet). As there are three triplet states and only one singlet, an experiment where the nucleons are not polarized will register three times more events of the first type than of the second, resulting for the cross section the combination

$$\sigma = \frac{3}{4}\sigma_t + \frac{1}{4}\sigma_s. \tag{2.129}$$

If then $\sigma = 20.4$ b and $\sigma_t = 3.4$ b, one gets for σ_s the value 71 b! The explanation for this high value is found in the fact that the singlet potential is shallower than the triplet one, being within the threshold for the appearance of the first bound state. This gives rise to a resonance when the incident particle has very low energy, as happens in the present case.

There are ways to find whether the singlet potential has a bound state with a very low negative energy or if the resonance occurs at a very low yet positive energy. For that let us initially study the scattering amplitude variation as a function of the well depth in the case of very low incident energy E. When $V_0 = 0$, (2.92) has the simple form $u'' = 0$, and the trivial solution for u is a straight line crossing the origin. When V_0 is small and forms the well, the form of the wavefunction looks like figure 2.8a. There is no bound state yet, and the scattering length a is negative (see 2.114). When V_0 is deep enough to allow the existence of the first bound state, the form of the wavefunction is as in figure 2.8b, with a maximum inside the well. This is an expected behavior: the internal part of the wavefunction is not sensitive to the fact that E is a little positive or negative, and a bound state wavefunction should have in r_0 a negative derivative to match to the exponential decay of the external part. The essential result is that the sign of a is, in this case, positive. Thus, the sign of the scattering length can show us if a resonance occurs with a negative (bound) state or a positive (virtual) energy.

The combination of (2.113) and (2.129) gives

$$\sigma = \pi(3a_t^2 + a_s^2), \tag{2.130}$$

where a_t and a_s are the scattering length for the triplet and singlet potentials, with respective cross sections σ_t and σ_s given by expressions such as (2.113). For an equation like (2.130) it does not matter what the sign of the scattering amplitude is, since it expresses an *incoherent* combination of singlet and triplet scattering. The cross section is proportional to the square of the amplitudes, in the same way as the intensity of a light beam is proportional to the square of the magnitude of the electric (or magnetic) field. One form of *coherent* scattering is achieved when the wavelength of the incident particles is of the order of the distance between the nuclei inside a molecule. In the case of neutrons incident on H_2, the distance between the protons in the molecule is about 0.8×10^{-8} cm and the coherent scattering is reached with a neutron energy near 2×10^{-3} eV. The scattering of these very slow neutrons by a hydrogen molecule produces an interference phenomenon similar to that occurring with light waves that emerge from the two slits of a Young experiment. An additional ingredient in the present case is that the H_2 molecule can be in two states, one with the spins of the protons forming a triplet (orthohydrogen) and the other where the spins form a singlet (parahydrogen). When a neutron interacts with an orthohydrogen molecule the two scattering amplitudes are of the same type; when the interaction is with parahydrogen they are of different types. Schwinger and Teller [ST37] have found expressions for the scattering cross sections of slow neutrons with ortho- and parahydrogen:

$$\sigma = c_1(a_t - a_s)^2 + c_2(3a_t + a_s)^2,\tag{2.131}$$

where c_1 and c_2 are numerical coefficients, with different values for the two types of hydrogen and also depending upon the incident neutron energy and the gas temperature. This last dependence is natural since the incident neutrons have very low velocities and the thermal molecular motion, in this case, has a non-negligible influence. As an example, at a temperature of 20.4 K and with 0.0045 eV neutrons the coefficients are, for orthohydrogen, $c_1 = 13.762$ and $c_2 = 6.089$, and for parahydrogen, $c_1 = 0$ and $c_2 = 6.081$. Note that in (2.131), contrary to (2.130), the signs of a_t and a_s are important for the calculation of σ.

From (2.131) it is possible to obtain the scattering lengths a_t and a_s if the experimental cross sections are known. Measurements of these cross sections using gaseous hydrogen have been done since 1940 [SS55], improving former work done with liquid H_2, where the effects due to the intermolecular forces are difficult to separate. The cross sections were measured from room temperature, where the proportion is 75% orthohydrogen and 25% parahydrogen, down to 20 K. At the lowest temperature only parahydrogen exists since it has a greater binding energy than orthohydrogen and can be formed by the decay of orthohydrogen, provided the process is accelerated by a catalyzer (a substance with paramagnetic atoms that induces the spin change of one of the protons of the H_2 molecule).

The results found for the scattering lengths in these and other experimental works using different methods are not free of some systematic errors. Houk [Ho71] recommended the values

$$a_t = (5.423 \pm 0.005) \text{ fm}, \quad a_s = (-23.71 \pm 0.01) \text{ fm}\tag{2.132}$$

for the scattering lengths. Note that these values also satisfy (2.130). The negative sign of the singlet scattering length is the answer to our question related to figure 2.8: the proton-neutron system has no bound state except the deuteron ground state. The resonance in the low energy scattering of neutrons by protons is due to a state of the system with a small positive energy.

2.10 Effective Range Theory

In the previous section we developed the theory of elastic scattering at energies close to zero, where the cross sections are expressed by (2.113). When the incident neutron energy goes beyond this limit we have two problems to face. First, the limit (2.112) is no longer applicable and the scattering length alone cannot determine the cross section. Second, the series (2.103) cannot be truncated in $l = 0$, since the terms $l = 1, l = 2, \ldots$ begin to have a significant contribution. In fact, this problem begins to be important only at energies of tens of MeV. The results that we shall obtain show that we can safely proceed up to 20 MeV using only the partial wave $l = 0$. The title of this section has thus the meaning that the zero energy approximation will no longer be valid but we will remain restricted to the $l = 0$ component of the angular momentum.

Our purpose is to investigate the behavior of the cross section (2.111) when we move away from the zero energy limit. The first results in this direction were established by Schwinger using a variational principle, but were reproduced afterward with a simpler method that is based only on the properties of the wavefunction. We will follow closely the work of H. Bethe [Bet49], where this method is explicated with clarity.

Let us consider the incident neutron with energy E_1 and wavenumber k_1. If we write (2.92) for $l = 0$ and use (2.121), the radial wavefunction satisfies

$$\frac{d^2 u_1}{dr^2} + k_1^2 u_1 - \frac{2m}{h^2} V(r) u_1 = 0.$$ (2.133)

For another energy E_2, we have

$$\frac{d^2 u_2}{dr^2} + k_2^2 u_2 - \frac{2m}{h^2} V(r) u_2 = 0.$$ (2.134)

Multiplying (2.133) by u_2 and (2.134) by u_1, subtracting and integrating, we arrive at

$$u_2 u_1' - u_1 u_2' \big|_0^R = (k_2^2 - k_1^2) \int_0^R u_1 u_2 \, dr,$$ (2.135)

where the limit R is arbitrary.

Let us define the function Ψ as the asymptotic form of u, but valid for every point in space:

$$\Psi_1 = \frac{\sin (k_1 r + \delta_1)}{\sin \delta_1}$$ (2.136)

where the normalization was chosen to make $\Psi = 1$ at the origin; this also determines the normalization of u. Note that the sub-index of the phase shift δ refers to the energy and not to the angular momentum.

A relation analogous to (2.135) is valid for Ψ:

$$\Psi_2 \Psi_1' - \Psi_1 \Psi_2'|_0^R = (k_2^2 - k_1^2) \int_0^R \Psi_1 \Psi_2 \, dr. \tag{2.137}$$

Let us subtract (2.135) from (2.137). If R is chosen beyond the range of the nuclear forces, where Ψ and u coincide, the contribution of the left side in the limit R will be zero. At the lower limit $u_1 = u_2 = 0$ and thus this term does not contribute. Extending the integration limit to infinity, we obtain:

$$\Psi_1(0) \Psi_2'(0) - \Psi_2(0) \Psi_1'(0) = (k_2^2 - k_1^2) \int_0^\infty (\Psi_1 \Psi_2 - u_1 u_2) \, dr. \tag{2.138}$$

The derivatives of (2.138) are obtained from (2.136), resulting in

$$k_2 \cot \delta_2 - k_1 \cot \delta_1 = (k_2^2 - k_1^2) \int_0^\infty (\Psi_1 \Psi_2 - u_1 u_2) \, dr. \tag{2.139}$$

Let us now apply (2.139) to the special case $k_1 = 0$. In this case, $k_1 \cot \delta_1 = -1/a$, where a is the scattering length. Ignoring the lower index 2, (2.139) can be rewritten as

$$k \cot \delta = -\frac{1}{a} + k^2 \int_0^\infty (\Psi_0 \Psi - u_0 u) \, dr. \tag{2.140}$$

No approximation has been done up to now and (2.140) is exact. But, looking at the integrand of (2.140), we see that it is different from zero inside the range of the nuclear forces; in this situation, Ψ and u depend very weakly on the energy. since E is supposedly small compared to $V(r)$ (see 2.92). A reasonable approximation is therefore to replace Ψ and u by Ψ_0 and u_0, respectively, and to write

$$k \cot \delta = -\frac{1}{a} + \frac{1}{2} k^2 r_{\text{eff}}, \tag{2.141}$$

with

$$r_{\text{eff}} = 2 \int_0^\infty (\Psi_0^2 - u_0^2) \, dr. \tag{2.142}$$

The quantity r_{eff}, which has the dimension of length. does not depend on the energy and is called *effective range*. The factor 2 was inserted in its definition to make it resemble the potential range. Gathering (2.111) and (2.141), we can express the cross section by

$$\sigma = \frac{4\pi}{k^2} \frac{1}{1 + \cot^2 \delta_0} = \frac{4\pi a^2}{a^2 k^2 + (1 - \frac{1}{2} a r_{\text{eff}} k^2)^2}. \tag{2.143}$$

where the influence of the potential is represented by two parameters, the effective range r_{eff} and the scattering length a. Thus the cross section is not affected by the details of the form of the potential since with any other reasonable form it will be always possible to adjust the depth and the range in such a way as to reproduce the values of a and r_{eff}. The result is that a study of low energy scattering does not lead to information about the form of the nucleon-nucleon potential. The theory of effective range is therefore sometimes called the *form independent approximation*.

For the application of the cross section (2.143) we have to remember that there are in fact two potentials, one for the singlet and another for the triplet state, and (2.143) should be, using (2.129), more appropriately written

$$\sigma = \frac{3}{4} \frac{4\pi a_t^2}{a_t^2 k^2 + (1 - \frac{1}{2} a_t r_t k^2)^2} + \frac{1}{4} \frac{4\pi a_s^2}{a_s^2 k^2 + (1 - \frac{1}{2} a_s r_s k^2)^2} . \tag{2.144}$$

implying the existence of four parameters to be determined: a_t, a_s, r_t, r_s, namely, the scattering lengths in the singlet and triplet states and the respective effective ranges. For the first two we have the established values (2.132). The effective range in the triplet state, r_t, can be obtained from well-known experimental information, the deuteron binding energy. For that goal it is enough to see that there is no restriction to employing the above theory to negative energies, namely, bound states. So let us use for u the deuteron radial wavefunction; in this case Ψ is the decreasing exponential (2.39),

$$\Psi = e^{-\sqrt{2mE_B}\, r/\hbar}. \tag{2.145}$$

already properly normalized. E_B is the deuteron binding energy and m its reduced mass. Using (2.138), with $\Psi_2 = \Psi$ and $\Psi_1 = \Psi_0$, we have

$$-\frac{\sqrt{2mE_B}}{\hbar} + \frac{1}{a_t} = -\frac{2mE_B}{\hbar^2} \frac{r_t}{2}. \tag{2.146}$$

being an expression that allows us to deduce r_t from a_t and E_B. The sign of the right-hand side of (2.146) was introduced because in the case of negative energy the sign of the second term of (2.134) should be changed. Using the values of (2.25) and (2.132), we get the effective range for the triplet potential:

$$r_t = 1.76 \text{ fm}. \tag{2.147}$$

The value of r_s cannot be obtained as a direct result of an experiment and is normally used in (2.144) as the parameter that best reproduces experimental values of the cross section. The value

$$r_s = 2.56 \text{ fm} \tag{2.148}$$

produces cross sections with (2.144) that are in very good agreement with experiment, as we can see in figure 2.7.

2.11 Proton-Proton Scattering

This type of scattering is more difficult to deal with than that of the neutron-proton case. Aiming to pinpoint the origin of some difficulties, we shall initially describe the essential differences between the two types of scattering.

1) In p-p scattering there is a repulsive *Coulomb force* between the protons in addition to the nuclear force. The Coulomb forces are of long range: the differential cross section (Rutherford formula) diverges for small angles and the total cross section is infinite.

2) When we deal with identical particles, the Pauli principle puts restrictions on the spatial and spin wavefunctions. In particular, at low energies ($l = 0$), the spatial part is
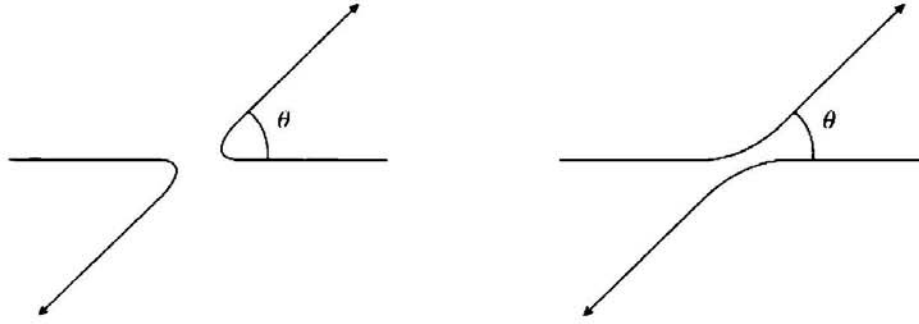
Figure 2.9 Two possible and indistinguishable ways to detect a proton in the angle θ after p-p scattering

symmetric and the spin part is, as a consequence, antisymmetric. In this way only the singlet state contributes to the cross section.

3) The indistinguishability between the protons implies that it is not possible to discriminate the two situations shown in figure 2.9. The wavefunction and the scattering amplitude should have contributions of θ and $\pi - \theta$. In the calculation of cross sections (square of the scattering amplitude) interference terms between the two parts show up. This is a purely quantum phenomenon, with no analog in classical physics.

4) The two independent forces, the nuclear and the Coulomb, contribute their own terms to the cross section. But, the nuclear scattering acts coherently with the Coulomb one and an interference term between the two effects also appears in the cross section.

To take care of all these questions the differential cross section (2.86) is composed of several parts. Its expression for the s-wave ($l = 0$), which we present without demonstration (see [BD04]), can be written as the sum

$$\frac{d\sigma}{d\Omega} = \left[\left(\frac{d\sigma}{d\Omega}\right)_c + \left(\frac{d\sigma}{d\Omega}\right)_n + \left(\frac{d\sigma}{d\Omega}\right)_{cn} \right]. \tag{2.149}$$

The first two terms of (2.149) are due to the Coulomb and nuclear potential, respectively, and the third is the interference term between them. Explicitly (see [BD04]),

$$\left(\frac{d\sigma}{d\Omega}\right)_c = \left(\frac{e^2}{2E_p}\right)^2 \left\{ \frac{1}{\sin^4(\theta/2)} + \frac{1}{\cos^4(\theta/2)} - \frac{\cos\left\{\eta \ln\left[\tan^2(\theta/2)\right]\right\}}{\sin^2(\theta/2)\cos^2(\theta/2)} \right\}, \tag{2.150}$$

where $e^2 = 1.44$ MeV $\cdot$ fm, E_p is the kinetic energy of the incident proton in the laboratory system, assuming the second proton to be at rest, θ is the scattering angle in the center of mass system, and $\eta = e^2/(\hbar v)$, v is the relative velocity between the protons. The first term in (2.150) refers to the usual Rutherford scattering; the second is due to the necessary existence of a term in $\pi - \theta$ explained in item 3 above. The last term is the interference term between the two previous contributions, namely, the Coulomb scattering in θ and in $\pi - \theta$. This term was first studied by Mott [Mo30] and the full expression (2.150) is known as *Mott scattering*.

The term in (2.149) due to the nuclear potential has the expected form

$$\left(\frac{d\sigma}{d\Omega}\right)_n = \frac{\sin^2\delta_0}{k^2} \tag{2.151}$$
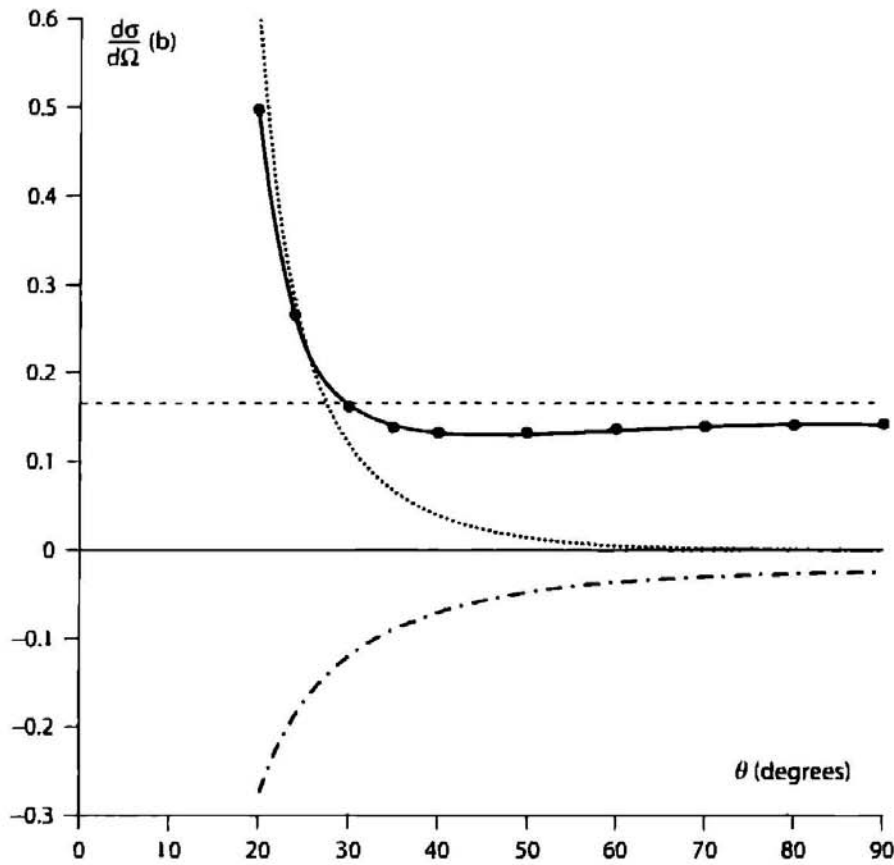
Figure 2.10 Composition of the proton-proton differential scattering cross section (solid line) by the sum of Coulomb (dotted line) and nuclear (dashed line) parts and the interference term (dashed-dotted line). The energy of the incident protons is 3.037 MeV. The experimental points were taken from [Kn66] and the best fit to (2.149) is obtained with $\delta_0 = 50.952°$. Due to the symmetry about $90°$, only values up to this angle are shown.

and is written as a function of a pure nuclear phase shift δ_0. Since the nuclear scattering is isotropic, integration of (2.151) yields trivially the result (2.111). It remains to explain the interference term between the Coulomb and nuclear scattering:

$$\left(\frac{d\sigma}{d\Omega}\right)_{rn} = -\frac{1}{2}\left(\frac{e^2}{E_p}\right)^2\frac{\sin\delta_0}{\eta}\left\{\frac{\cos\left[\delta_0 + \eta\ln\sin^2(\theta/2)\right]}{\sin^2(\theta/2)} + \frac{\cos\left[\delta_0 + \eta\ln\cos^2(\theta/2)\right]}{\cos^2(\theta/2)}\right\}. \quad (2.152)$$

The nuclear phase shift δ_0 of (2.151) and (2.152) should be found by a best fit of (2.149) to the experimental points at each energy. In the example of figure 2.10 one obtains $\delta_0 = 50.952°$ for $E_p = 3.037$ MeV. We also see in the figure that the interference yields a total cross section that can be smaller than the purely Coulomb or nuclear part.

When the above procedure is repeated for several energies one obtains the graph in figure 2.11. Note that the interference term allows one to obtain the sign of δ_0 from the experimental cross sections, which is not possible with low energy neutron-proton scattering (see 2.151).

In the study of neutron-proton scattering we developed the effective range theory, where the phase shifts have their values linked to only two parameters connected to the potential,
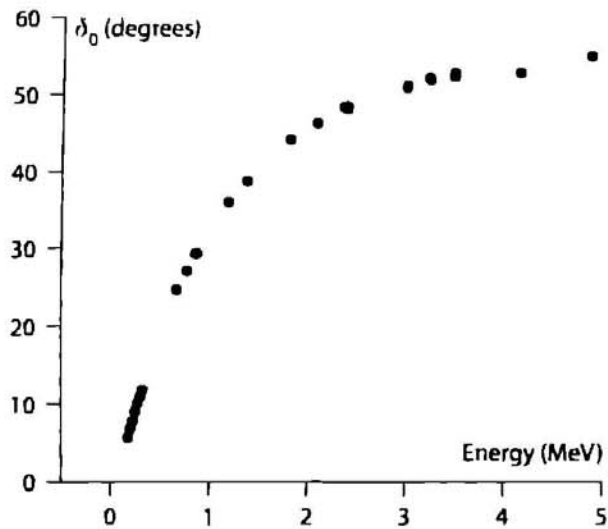
Figure 2.11 Phase shift variation as a function of the incident proton energy for proton-proton collision. The experimental points are from reference [JB50].

not depending on details about the form of the potential. The application of a form-independent theory to the case of proton-proton scattering demands some care, since the Coulomb potential has infinite range and even in the zero energy limit the approximation (2.141) is no longer valid. Despite this, a theory for the process was developed [JB50], resulting in parameters comparable to the scattering length and to the effective range of the neutron-proton singlet scattering. For proton-proton scattering we have

$$a_s = (-7.82 \pm 0.01) \text{ fm}, \quad r_s = (2.79 \pm 0.02) \text{ fm}. \tag{2.153}$$

The much lower absolute value of a_s now found is not of great significance in comparative terms because the Coulomb force adds to the nuclear one. There are means, however, to approximately subtract the effect of this force [JB50] and to evaluate proton-proton scattering amplitudes as if there were only the nuclear force. This new value is $a_s \cong -17$ fm, closer to but yet different from the value corresponding to neutron-proton scattering ($a_s = -23.71$ fm). It is still an open question whether this difference is real or caused by deficiency in the methods, but, anyway, an examination of figure 2.8 show us that a difference like this has little influence on the wavefunction. Similar values for the parameters of neutron-proton and proton-proton collisions would support the assumption of charge independence of the nuclear force, and with the available results we can say that at least approximately this assumption is true.

2.12 Neutron-Neutron Scattering

Low energy neutron-neutron scattering does not present any additional theoretical difficulty as compared to neutron-proton scattering, since in both cases the nuclear force is

the only agent. The problem here is of experimental character, since a neutron target is not available and the study of the interaction should be done indirectly.

One of the methods employed consists in analyzing the energy spectrum of the protons resulting from the reaction

$$n + d \rightarrow p + n + n. \tag{2.154}$$

It is a continuous spectrum but presents a peak near the maximum energy. This indicates a resonance related to the formation of the *di-neutron* virtual state, and the peak width can give information about the scattering length. When one collects this and other results from reactions with two neutron formation, one can extract the average values

$$a_s = (-17.6 \pm 1.5)\ \text{fm}, \quad r_s = (3.2 \pm 1.6)\ \text{fm} \tag{2.155}$$

for the scattering length and effective range of the neutron-neutron scattering, respectively. These values are closer to the proton-proton nuclear scattering than to the neutron-proton scattering. Hence, since they are stronger than the charge independence, there is the indication of a *charge symmetry* of the nuclear force.

2.13 High Energy Scattering

When the energy of the incident nucleon reaches some tenths of an MeV, new modifications in the elastic scattering treatment are necessary: waves with $l > 0$ begin to be important and the differential cross section, according to (2.88) and (2.103), will be determined by the interference of different l values. If, for example, $l = 0$ and $l = 1$ waves are present in the scattering, then

$$\frac{d\sigma}{d\Omega} = \frac{1}{k^2} \left[\sin^2 \delta_0 + 6 \sin \delta_0 \sin \delta_1 \cos (\delta_0 - \delta_1) \cos \theta + 9 \sin^2 \delta_1 \cos^2 \theta \right]. \tag{2.156}$$

As a consequence, the interference between s and p scattered waves leads to breaking the scattering symmetry about the angle $\theta = 90°$ that would exist if each wave scattered independently.

Up to an energy close to 280 MeV, elastic scattering is the only process to occur in a nucleon-nucleon collision. The nucleons do not have low energy excited states and the weak interaction (chapter 8) is very slow to manifest itself in a scattering process. Figure 2.12 sketches proton-proton total cross section behavior as a function of energy. The smooth decrease in energy is interrupted at 280 MeV (135 MeV in the center of mass), value that sets the threshold of pion creation. With the beginning of the contribution of these inelastic processes, the total cross section separates from the elastic one.

2.14 Laboratory and Center of Mass Systems

With the aim of completing the elastic scattering study, we will see in this section how the change in the reference frame affects the quantities related to the scattering, specially angular distributions.
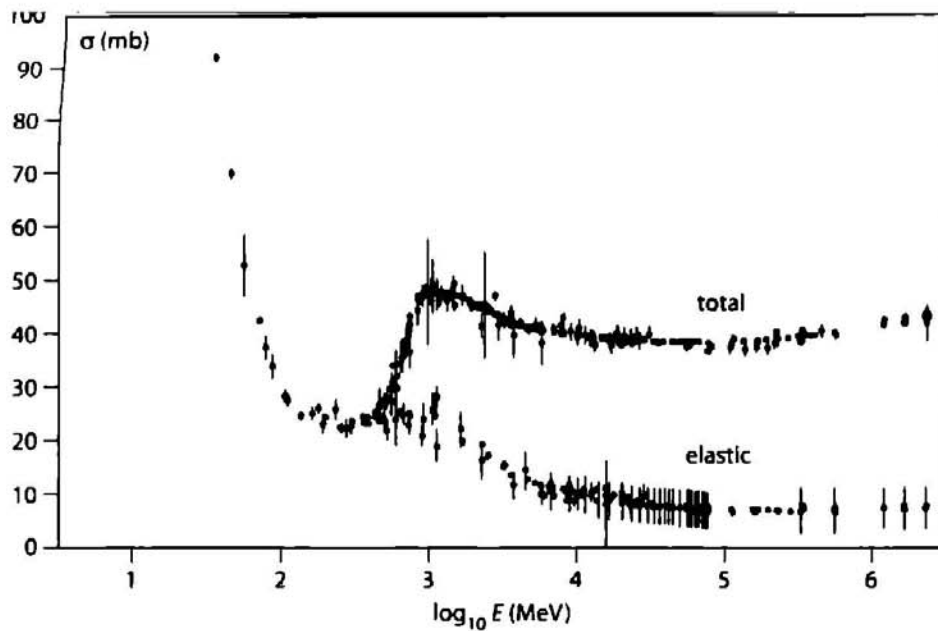
Figure 2.12 Total and elastic proton-proton cross sections as a function of the laboratory energy [Ba96].

The center of mass of a system of particles is defined by the vector

$$\mathbf{r}_c = \frac{\sum m_i \mathbf{r}_i}{\sum m_i}, \tag{2.157}$$

which moves with the velocity

$$\mathbf{v}_c = \frac{\sum m_i \mathbf{v}_i}{\sum m_i}. \tag{2.158}$$

In the special case of two particles with the second at rest, the center of mass velocity has the simple expression

$$V_c = \frac{m_1 V}{m_1 + m_2} = V \frac{m_R}{m_2}, \tag{2.159}$$

where V is the velocity of particle 1 and m_R the system reduced mass, defined by

$$m_R = \frac{m_1 m_2}{m_1 + m_2}. \tag{2.160}$$

Figure 2.13 shows this collision as seen by an observer located at the center of mass. One sees that the total linear momentum is always zero when computed at the center of mass. This property can be used to make it easier to evaluate the energy balance of a reaction. From the laboratory point of view, one should add the center of mass velocity to the velocities of figure 2.13. The result is seen in figure 2.14: θ and ϕ are the emerging angles of particles 1 and 2 (the latter being initially at rest), respectively. The triangle ABC
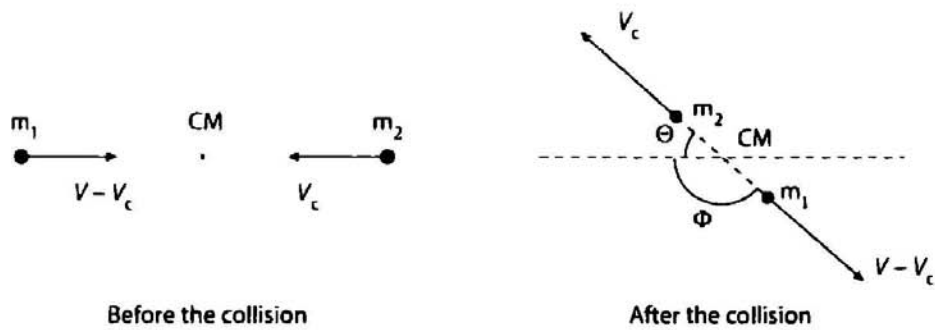
Figure 2.13 Collision seen by an observer located at the center of mass.

is isosceles; hence $\Phi - \phi = \phi$ and thus

$$\phi = \frac{1}{2}\Phi = \frac{1}{2}(\pi - \Theta), \tag{2.161}$$

relations that are independent of m_1 and m_2. In the triangle CDE,

$$\cot\theta = \frac{CD}{DE} = \frac{V_c + (V - V_c)\cos\Theta}{(V - V_c)\sin\Theta} = \frac{V_c/(V - V_c) + \cos\Theta}{\sin\Theta} = \frac{m_1/m_2 + \cos\Theta}{\sin\Theta}; \tag{2.162}$$

thus

$$\cot\theta = \frac{m_1}{m_2}\csc\Theta + \cot an\Theta. \tag{2.163}$$

Relations (2.161) and (2.163) define how the angles change in the passage from one system to the other.

The differential cross sections $\sigma(\theta)$ and $\sigma(\Theta)$ can also be related. For that, we have to keep in mind that if ω and Ω are the solid angles associated to θ and Θ, respectively, then $\sigma(\theta)d\omega = \sigma(\Theta)d\Omega$, since the detected particles are the same in both cases (see definition
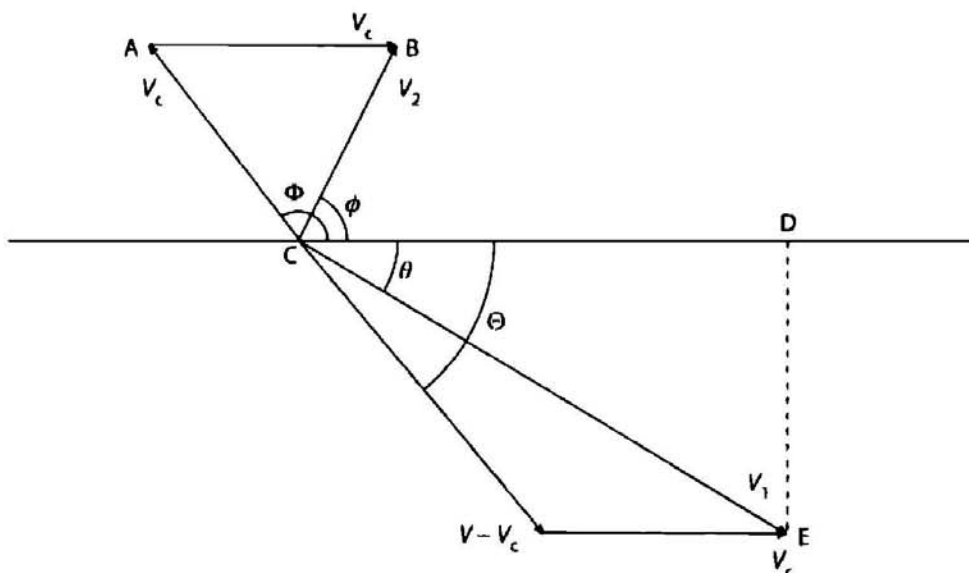

Figure 2.14 Transformation of center of mass velocities to the laboratory.

2.86). In this way

$$\frac{\sigma(\theta)}{\sigma(\Theta)} = \frac{d\Omega}{d\omega} = \frac{2\pi \sin \Theta \, d\Theta}{2\pi \sin \theta \, d\theta}. \tag{2.164}$$

Using now (2.163) to obtain $d\Theta/d\theta$, we get

$$\frac{\sigma(\theta)}{\sigma(\Theta)} = \frac{\sin^3 \Theta}{\sin^3 \theta} \left(\frac{1}{1 + m_1 \cos \Theta / m_2} \right), \tag{2.165}$$

which is the relation between the cross sections in the two systems that we were searching for.

2.15 Exercises

1. Use the listed values for the masses of the proton, neutron, and deuteron and deduce the value (2.25) for the binding energy of the deuteron.

2. Calculate the percent loss of mass due to the binding energy for the systems: a) earth-moon; b) hydrogen atom; c) deuteron. Verify that only in the last case is this effect important.

3. Using (2.36) and (2.39) as the wavefunction of the deuteron, calculate: a) the fraction of time that the neutron and the proton spend out of range of the force between them; b) the mean square radius of the deuteron.

4. A common generalization of the potential of figure 2.1 is the addition of a "hard core," that is, $V = +\infty$ for $r < c$, c being the radius of the core. Show that the presence of the core modifies the wavefunctions but does not alter the relationship between E_B, R, and V_0 given by (2.43).

5. Suppose that the interaction potential between the neutron and the proton is exponential, of the form $V = V_0 e^{-r/2r_n}$, where V_0 and r_n are, respectively, the depth and range of the nuclear potential. a) Write the Schrödinger equation (in the center of mass system) for the ground state of the deuteron, of angular momentum $l = 0$. b) Use the definition $x = e^{-2r/r_n}$ and $\psi(r) = u(r)/r$. Show that the Schrödinger equation has a Bessel function as solution. Write the general solution of this equation. c) Applying the boundary conditions (ψ finite for $r = 0$ and $r = \infty$), determine the relationship between V_0 and r_n.

6. For a system of two nucleons, show that $L + S + T$ should be odd, where L, S, and T are, respectively, the quantum numbers of orbital momentum, spin, and isospin of the system.

7. The deuteron has spin 1. What are the possible states of total spin and total angular momentum of two deuterons in a state with orbital angular momentum L?

8. Suppose that the meson π^- (spin 0 and negative parity) is captured from the orbit P in a pionic atom, giving rise to the reaction

$$\pi^- + d \longrightarrow 2n. \tag{2.166}$$
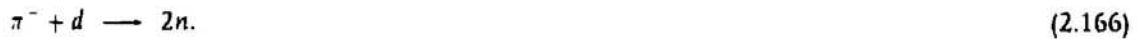
Show that the two neutrons should be in a singlet state.

9. Show that if $S_l(k)$ has the form (2.100), the wavefunction (2.99) describes an elastic scattering. Suggestion: show that the flux of the probability current vector through a sphere that involves the scattering center is zero.

10. Demonstrate the relation (2.103), using (2.82), (2.98), and (2.99).

11. Demonstrate the relation (2.104), using (2.103) and

$$\int d\Omega \, P_l(\cos\theta) \, P_{l'}(\cos\theta) = \frac{4\pi}{2l+1} \, \delta_{ll'} \,. \tag{2.167}$$

12. Find the cross section for low energy particles incident in a "hard sphere" potential

$$V(r) = \infty \quad (r < R). \tag{2.168}$$

$$V(r) = 0 \quad (r > R). \tag{2.169}$$

13. Low energy neutrons are scattered by protons. Let θ and ϕ be the emerging angles of neutrons and protons, respectively. a) Show that, for a given event, $\theta + \phi = 90°$. b) The scattering is isotropic in the center of mass and (2.165) shows that the neutron angular distribution in the laboratory system is given by $\sigma(\theta) = 4\cos\theta \, \sigma(\Theta)$. Show that for protons there is the relationship $\sigma(\phi) = 4\cos\phi \, \sigma(\Phi)$. c) Since $\sigma(\Theta)$ and $\sigma(\Phi)$ are constants, the functions $\sigma(\theta)$ and $\sigma(\phi)$ have maxima in $0°$. How does this result harmonize with the result of item (a)?

14. Say why it is not possible for a proton at rest to scatter another proton of low energy if both spins have the same direction.

15. A neutron of kinetic energy E_1 is elastically scattered by a nucleus of mass M, remaining with a final kinetic energy E_2. a) With Θ the scattering angle in the center of mass, show that

$$\frac{E_1}{E_2} = \frac{1}{2}\left[(1+\alpha) - (1-\alpha)\cos\Theta\right]. \tag{2.170}$$

where $\alpha = |(M-1)/(M+1)|^2$. b) What is the maximum loss of kinetic energy as a function of E_1 and M? For which angle Θ does it occur? Which angle θ in the laboratory system corresponds to this value of Θ?

16. Assume that, in the scattering of a particle by a central potential, all phase shifts δ_l except for δ_0 and δ_1 are negligibly small.

(a) Find the differential and total (integrated over angles) cross sections.

(b) For $\delta_0 = 20°$ and $\delta_1 = 2°$ calculate the relative contribution of the p-wave to the total cross section and the ratio of cross sections in the forward, $\theta \to 0$, and in the backward, $\theta \to \pi$, directions.

17. Consider the *Born approximation* scattering amplitude (see [BD04])

$$f(\mathbf{k}', \mathbf{k}) = -\frac{m}{2\pi\hbar^2} \int d^3r\, e^{-i(\mathbf{k}'\cdot\mathbf{r})} U(\mathbf{r}) e^{i(\mathbf{k}\cdot\mathbf{r})} \tag{2.171}$$

for the spherically symmetric potential $U(r)$.

(a) Using in (2.171) the expansion of the plane wave over spherical waves and the addition theorem for spherical harmonics (see Appendix A), present the scattering amplitude as an expansion over Legendre polynomials of the angle ϑ between $\mathbf{k}$ and $\mathbf{k}'$ and find the partial amplitudes f_l.

(b) For the short-range potential of radius R, $kR \ll 1$, and typical magnitude $\bar{U}$, estimate the energy dependence of the phase shifts δ_l.

18. Which of the following quantities are conserved? Energy E, components of the momentum $\mathbf{p}$, components of the orbital momentum $\mathbf{l}$, its square $\mathbf{l}^2$, parity $\mathcal{P}$, when a particle is moving

(a) with no external fields (free motion);

(b) in the static uniform field along the z direction;

(c) in the static central field $U(r)$;

(d) in the field $U = f(\rho)$ where ρ is the radius in the x, y-plane;

(e) in the uniform field along the x-direction with time-dependent amplitude?

19. The nucleus of the deuterium atom (heavy hydrogen isotope) is the deuteron, the only existing bound state of a neutron + proton system, with binding energy $E_B = 2.2$ MeV.

(a) Assuming that the orbital momentum of relative motion in the deuteron is $l = 0$, calculate the penetration length $1/\kappa$ of the deuteron wave function in the classically forbidden region outside the nuclear potential (see problem 3).

(b) Consider the neutron-proton potential as a square well of radius $R = 1.7$ fm (1 fm = 10^{-13} cm). Calculate the critical depth for the appearance of a bound state in this well.

(c) For a bound state with a small but nonzero binding energy ϵ, the square potential has to be deeper compared to its critical depth U_0^{crit} by $\delta U_0 = U_0 - U_0^{crit}$. Considering the matching conditions for a well slightly deeper than the critical one, $\delta U_0 \ll U_0^{crit}$, derive the connection between δU_0 and ϵ and calculate the depth of the potential for the deuteron (the radius value is given in part b).

(d) Estimate the probability for the proton and the neutron in the deuteron to be outside the region $r < R$ of nuclear attraction.